Pharmacophore-Based Design of Sphingosine 1-phosphate-3 Receptor Antagonists That Include a 3,4-Dialkoxybenzophenone Scaffold

Yuuki Koide,*[,†,§] Kazuhiro Uemoto,[†] Takeshi Hasegawa,[†] Tomoyuki Sada,[†] Akira Murakami,[†] Hiroshi Takasugi,[†,‡] Atsuko Sakurai,[‡] Naoki Mochizuki,[‡] Atsuo Takahashi,[†] and Atsushi Nishida[§]

Drug Research Department, Tokyo Research Laboratories, TOA EIYO Ltd., 2-293-3 Amanuma, Oomiya, Saitama 330-0834, Japan, Department of Structural Analysis, National Cardiovascular Center Research Institute, 5-7-1 Fujishirodai, Suita, Osaka 565-8565, Japan, and Graduate School of Pharmaceutical Sciences, Chiba University, 1-33 Yayoi, Inage, Chiba 263-8522, Japan

Received July 16, 2006

Sphingosine 1-phosphate (S1P) receptors are G-protein-coupled receptors. Among the five identified subtypes $S1P_1$−5, the $S1P_3$ receptor expressed on vascular endothelial cells has been shown to play an important role in cell proliferation, migration, and inflammation. A pharmacophore-based database search was used to identify a potent scaffold for an $S1P_3$ receptor antagonist by common feature-based alignment and further validated using the Güner−Henry (GH) scoring method. Assumed excluded volumes were merged into this model to evaluate the steric effect with the $S1P_3$ receptor. Three commercially available compounds were identified as $S1P_3$ receptor antagonists, with IC_{50} values $<5\ \mu M$. The synthesis of further derivatives revealed that the 3,4-dialkoxybenzophenone scaffold is a potent component of an $S1P_3$ receptor antagonist. Our results indicate that pharmacophore-based design of $S1P_3$ receptor antagonists can be used to expand the possibility of structural modification through scaffold-hopping based on a database search.

Introduction

Sphingosine 1-phosphate (S1P[a]) is a potent lipid mediator produced from the metabolism of sphingomyelin (Figure 1). S1P acts on a family of G-protein-coupled receptors (GPCRs) and transduces intracellular signals involved in numerous cellular processes.[1,2] The $S1P_1$ receptor, which was the first S1P receptor to be identified, was initially named endothelium differentiation gene-1 (Edg-1) receptor.[3] The five subtypes of S1P-induced Edg receptors were renamed S1P receptors, consistent with the official IUPHAR nomenclature for rational classification; $S1P_1$ (formerly Edg-1), $S1P_2$ (formerly Edg-5), $S1P_3$ (formerly Edg-3), $S1P_4$ (formerly Edg-6), and $S1P_5$ (formerly Edg-8).[4]

$S1P_3$ receptors expressed on vascular endothelial cells play several important roles, such as in cell proliferation based on extracellular signal-regulated kinase (ERK) activation in a pertussis toxin (PTX)-sensitive manner,[5] developmental and pathological angiogenesis,[6] endothelial cell migration,[7] and the activation of eNOS.[8] The role of vascular $S1P_3$ receptors has been reviewed in detail.[9−12]

The advent of the novel immunosuppressant **2** has inspired considerable interest in agonists and antagonists of S1P receptors (Figure 1).[13] It has been demonstrated that **2** is metabolized across various species to a monophosphate ester **3**, which is a high-affinity ligand for $S1P_1$, $S1P_3$, $S1P_4$, and $S1P_5$, but not $S1P_2$.[14,15] Administration of **2** resulted in the sequestration of circulating lymphocytes within secondary lymphoid tissues. Its egress-blocking effect occurs through the inactivation of the $S1P_1$ receptor.[16] Therefore, an $S1P_1$ receptor-selective agonist or antagonist has been expected to be a more effective immunosuppressant than **2**.

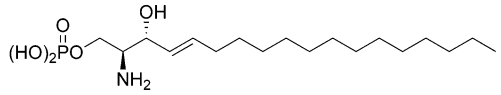

Sphingosine 1-phosphate (S1P) **1**

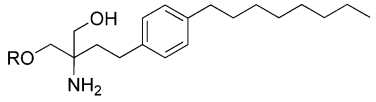

R = H **2** (FTY720)
R = -P(=O)(OH)$_2$ **3** (FTY720 phosphate (FTY720-P))

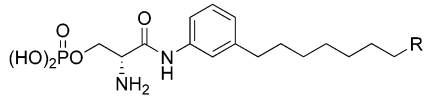

R = Me **4** (VPC23019)
R = H **5** (VPC25239)

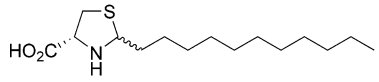

(4*R*)-4-Undecylthiazolidine-2-carboxylic acid **6**

Figure 1. S1P, reported $S1P_1$ receptor agonists and $S1P_3$ receptor antagonists (**3**, $S1P_{1,\ 3-5}$ receptor agonist; **2**, immunosuppressant which is the precursor for **3**; **4** and **5**, $S1P_1$/$S1P_3$ receptor antagonists; **6**, $S1P_3$ receptor antagonist.).

Clinical studies with **2** have identified dose-dependent transient symptomatic bradycardia in stable renal transplant patients.[17] Bradycardia is consistent with the S1P-induced activation of muscarinic receptor-activated inwardly rectifying K^+ current ($I_{K.Ach}$).[18−20] Recent studies in $S1P_3$ null mice have shown that the induction of bradycardia is mediated through the activation of $S1P_3$ receptors.[21,22] Meanwhile, $S1P_2$ and $S1P_3$, which are abundantly expressed in airway smooth muscle

* To whom correspondence should be addressed. Tel: +81(48)6477971. Fax: +81(48)6480078. E-mail: koide.yuuki@toaeiyo.co.jp.
† TOA EIYO Ltd.
‡ National Cardiovascular Center Research Institute.
§ Chiba University.

[a] Abbreviations: S1P, sphingosine 1-phosphate; EDG, endothelium differentiation gene; GH score, Güner−Henry score.

10.1021/jm060834d CCC: $37.00
Published on Web 01/11/2007

(ASM), mobilize calcium and mediate airway hypercontractility.[23] Administration of **2** induces bronchoconstriction and elevates airway constriction, while administration of an $S1P_1$ receptor-selective agonist has no effect on bradycardia or airway resistance.[24,25]

Taken together, these results suggest that an $S1P_3$ receptor antagonist may be useful for preventing vascular proliferation, bradycardia, and bronchoconstriction. Furthermore, elucidation of the structural requirements for $S1P_3$ receptor antagonist may enable the development of a more selective $S1P_1$ receptor antagonist. While several $S1P_1$ receptor-selective agonists have been reported, there have been few reports on $S1P_3$ antagonists.[26] Although suramin has been reported to be an $S1P_3$ receptor-selective antagonist, it also acts as a reversible *P*2-purinoceptor antagonist,[27,28] an inhibitor of DNA topoisomerase II,[29] and a potent inhibitor of the reverse transcriptase of RNA tumor viruses.[30] Suramin has also been reported to act as a direct antagonist of heterotrimeric G proteins.[31] Recently, practical $S1P_1$/$S1P_3$ receptor antagonists **4** and **5**, which have meta-alkylated phenyl structures, were reported from the University of Virginia (Figure 1).[32,33] However, the activities of these antagonists toward $S1P_3$ receptors are at least one-fifth less than those toward $S1P_1$ receptors.

To identify structurally novel agonists or antagonists efficiently, a computational approach for scaffold-hopping has been extensively applied.[34] Structure-based virtual screening, in which the 3D structure of a target protein (usually derived from X-ray crystallography) is used in protein−ligand docking calculations, has been used extensively to explore potent compounds. However, this approach to scaffold-hopping in GPCRs is limited due to issues involving purification and crystallization. Meanwhile, a pharmacophore is a generic description of the key features of an active molecule and is usually built by overlaying different conformations of active compounds. Pharmacophore models derived from active ligands have been widely used to explore GPCR ligands.[35]

We developed 2-alkyl or aryl thiazolidine-4-carboxylic acid derivatives as potent $S1P_3$ antagonists at 10 μM by a pharmacophore-based database search which included information on the conformations of S1P.[36] However, very recently, one of these compounds, (4*R*)-4-undecylthiazolidine-2-carboxylic acid **6** (Figure 1), has been reported to be inappropriate for identifying selective antagonism at the $S1P_3$ receptor due to its low potency and reduced selectivity.[37] More potent and practical $S1P_3$ receptor antagonists are still needed.

We have continued to study more potent $S1P_3$ receptor antagonists, which may be useful for influencing vascular proliferation and inflammation, or at least for elucidating the detailed mechanism of $S1P_3$ receptor antagonism. In this report, we describe **(i)** the generation and assessment of a pharmacophore model for $S1P_3$ receptor antagonists, **(**ii**)** the identification of novel potent $S1P_3$ antagonists retrieved from among commercially available compounds by a pharmacophore-based database search, **(**iii**)** the structure−activity relationship of synthesized derivatives as $S1P_3$ receptor antagonists, and **(**iv**)** the structural requirements for $S1P_3$ receptor antagonists.

Methods

1. Generation and Validation of Pharmacophore Models. The scheme for generating reliable pharmacophore models for $S1P_3$ receptor antagonists is outlined in Chart 1. First, pharmacophore models were constructed by aligning active compounds as $S1P_3$ receptor antagonists with multiple conformations (training set). Second, the generated pharmacophore models were validated to identify preferable models that could be used to efficiently exclude inactive compounds. Third, information regarding steric properties was added to the pharmacophore models, since these models could not exclude inactive compounds which probably had decreased potency due to extreme molecular volumes. Finally, these modified pharmacophore models were validated if they made it possible to efficiently exclude inactive compounds and to identify active compounds that were not used for pharmacophore generation (test set). The most reliable pharmacophore model was then identified. The details of each step are described below.

Chart 1. Chart for Deriving a Pharmacophore Model of $S1P_3$ Receptor Antagonists

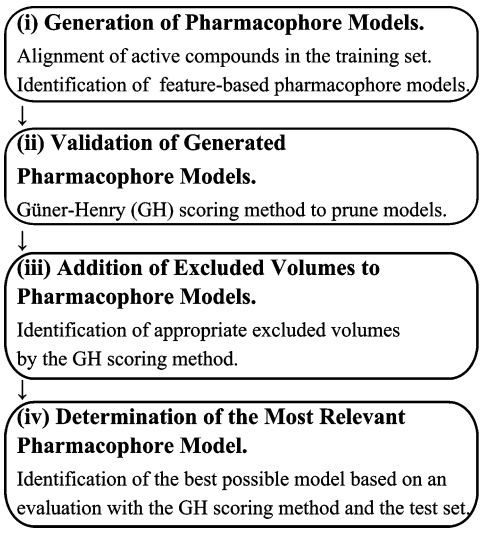

(i) Generation of the Pharmacophore Model. A feature-based pharmacophore model derived from the active compound set with diverse conformations without quantitative activity data was applied.[38] It describes possible pharmacophoric space as an arrangement of features. For example, a feature, such as *hydrogen-bond acceptor*, is described which defines the kind of interaction with the target protein.

In this paper, we used three common features: *hydrogen-bond acceptor*, *hydrophobic*, and *negative ionizable*. The *hydrophobic* feature matches the following types of groups of atoms: a contiguous set of atoms that are not adjacent to any concentrations of charge (charged atoms or electronegative atoms) in a conformer such that the atoms have surface accessibility, including phenyl, cycloalkyl, isopropyl, and methyl groups. The *hydrogen-bond acceptor* feature matches the following types of atoms or groups of atoms with surface accessibility: sp or sp^2 nitrogens that have a lone pair and charge less than or equal to zero, sp^3 oxygens or sulfurs that have a lone pair and charge less than or equal to zero, or nonbasic amines that have a lone pair. The *negative ionizable* feature matches atoms or groups of atoms that are likely to be deprotonated at physiological pH, such as trifluoromethyl sulfonamide hydrogens, sulfonic acids, phosphonic acids, sulfinic, carboxylic, or phosphinic acids, tetrazoles, or negative charges not adjacent to a positive charge.

(ii) Validation of the Quality of Generated Pharmacophore Models. The Güner−Henry (GH) scoring method[39−41] was used to assess the quality of pharmacophore models. The GH score is a metric for quantifying the precision of hits and the recall of actives mined from a database consisting of known actives and inactives (Chart 2). It is considered a relevant metric, since it takes into account both the percent yield of actives in a

Chart 2. Metrics for Analyzing Hit Lists by a Pharmacophore Model-Based Database Search[a]

$$\%\,A = \frac{H_a}{A} \times 100$$

$$\%\,Y = \frac{H_a}{H_t} \times 100$$

$$E = \frac{H_a / H_t}{A / D}$$

$$GH = \left(\frac{H_a\,(3A+H_t)}{4H_t\,A}\right)\left(1 - \frac{H_t - H_a}{D - A}\right)$$

[a] Ha, number of actives in the hit list (true positives); Ht, number of hits retrieved; A, number of active compounds in the database; D, number of compounds in the database; % A, ratio of actives retrieved in the hit list (precision); % Y, yield of actives (recall); E, enrichment of the concentration of actives by the model relative to random screening without any pharmacophoric approach; GH, Güner−Henry score.

database (% *Y*, recall) and the percent ratio of actives in the hit list (% *A*, precision). The GH score ranges from 0, which indicates the null model, to 1, which indicates the ideal model. On the basis of S1P-induced cytosolic Ca^{2+} mobilization in CHO cells expressing the $S1P_3$ receptor, a compound with more than 30% inhibitory activity at 10 μM was defined as an "active" and a compound with less than 20% inhibitory activity at 10 μM was defined as an "inactive". For GH score assessment, all compounds with inhibitory activities of 20 to 30% at 10 μM were excluded to simplify the classification.

(iii) Addition of Excluded Volumes to Pharmacophore Models. Steric interaction can be approximated by the strategic placement of excluded volumes (spheres that cannot be penetrated by the ligand) in the pharmacophore model. The inclusion of excluded volumes in pharmacophore models has been reported to improve the pruning of database hit lists by 30−75%.[42] To obtain a more desirable pharmacophore model, appropriate excluded volumes were added by the GH scoring method.

(iv) Determination of the Most Relevant Pharmacophore Model. Pharmacophore models with excluded volumes were validated to identify the most relevant model by the same GH scoring method as described in section ii. In addition, pharmacophore models that could not identify any compound in the test set were excluded.

2. Database Searches. Composite databases, which contained a total of approximately three million commercially available compounds, were searched using the pharmacophore model. Hit compounds (hit list) can be ranked according to the fit value, which is the degree of consistency with the pharmacophore model. In this paper, the fit value is defined as the relative percentage compared to the maximum fit value. To decrease the number of hits, a minimum fit value, which is the lowest limit to qualify as a hit compound, was applied. In this paper, we used 90% of the minimum fit value to prune the hit list.

3. Biological Assay. The IC_{50} values for $S1P_1$, $S1P_2$, and $S1P_3$ receptors were quantitatively determined in terms of the Fura-2 fluorescent intensity. Dye was loaded into CHO cells that stably expressed $S1P_1$, $S1P_2$ or $S1P_3$ receptors. After addition of an antagonist, the inhibition of the transient increase in the intracellular calcium ion concentration ($[Ca^{2+}]_i$) induced by S1P was measured.

Results and Discussion

1. Generation and Validation of Pharmacophore Models. **(i) Generation of Pharmacophore Models.** Pharmacophore models for $S1P_3$ receptor antagonists were generated using five of seven active compounds: **6**, **8**, **10**, **11** and **12**, which were previously identified (Figure 2).[36] Compounds **7** and **9** were used as the test set in validation. Twelve patterns of pharmacophore generation were applied, based on three major parameters (Table 1): **(i)** The number of maximum features applied in a pharmacophore model was varied from three to five. **(ii)** *Negative ionizable* and *hydrophobic* features were applied for the generation of all models. Meanwhile, models were separately generated with or without the *hydrogen-bond acceptor* feature, since it was not clear whether this feature was important. **(iii)** 2-Alkyl or aryl thiazolidine-4-carboxylic acid derivatives **6**, **8**, **10** and **11** in the training set are diastereomers at *C*2 ((2*R*)- and (2*S*)-isomer). This complication may hamper conformational analysis and subsequent pharmacophore generation. Therefore, two training sets that included (2*R*)-thiazolidine-4-carboxylic acid derivatives **6**, **8**, **10** and **11** or their (2*S*)-derivatives were used. Compound **12** was used in both training sets. As a result, these three conditions gave 307 pharmacophore models.

(ii) Validation of Generated Pharmacophore Models. The quality of pharmacophore models was assessed using the GH score as a metric to search a database that consisted of 100 inactive compounds and seven active compounds **6**-**12** (all of their structures are shown in the Supporting Information). Since the results of validation were strongly influenced by the quality of the database, the composition of the active and inactive compounds in the database is the predominant factor in GH score assessment. Thus, the inclusion of inactive compounds was limited according to the following criteria. **(A)** All inactive compounds should match at least three types of features (*negative ionizable*, *hydrophobic* and *hydrogen-bond acceptor* features), the same as active compounds, since an inactive compound without one of these features in a pharmacophore model is excluded easily and thus it cannot reflect its ability. **(B)** Eighteen inactive compounds with thiazolidine-4-carboxylic acid scaffolds were included to avoid obtaining a too-strict and rigid pharmacophore model that could identify only the thiazolidine scaffold as an $S1P_3$ receptor antagonist.

The following criteria were applied to identify desirable pharmacophore models: A GH score of more than 0.4 was used to limit the number of models by less than 50%. A recall value of more than 0.5 was used for desirable pharmacophore models. Three hundred seven pharmacophore models were analyzed in a scatter diagram between the GH score and the recall of active compounds (Figure 3). Plots were divided into four blocks by the above criteria. Most of the plots were in the lower squares, which indicated a GH score of less than 0.4 and that these were nonselective pharmacophore models. The upper-left square showed too-exclusive pharmacophore models that could only identify a few active compounds. Meanwhile, in the upper-right square (GH score of more than 0.4 and recall of 0.5), the pharmacophore models can selectively retrieve most active compounds. The seven pharmacophore models in this upper-right square, which fulfilled the criteria, were selected from among the 307 models (Figure 4).

Pharmacophore models R1, R2, R3, and R4 were generated by the training set that included (2*R*)-thiazolidine-4-carboxylic acid derivatives. Meanwhile, pharmacophore models S1, S2 and S3 were generated by the model that consisted of (2*S*)-derivatives. All seven models included four features: one *negative ionizable*, one *hydrogen-bond acceptor*, and two *hydrophobic* features.

(iii) Addition of Excluded Volumes to Pharmacophore Models by Considering the GH Score. Our previous study

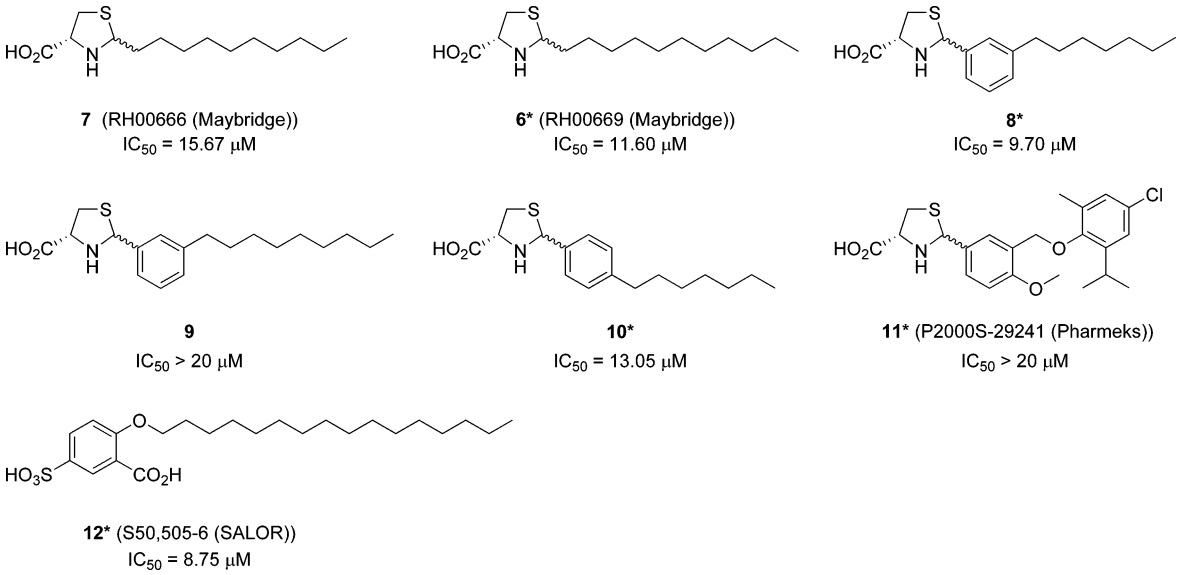

Figure 2. Previously identified $S1P_3$ receptor antagonists. Commercially available compounds are shown by the catalog number with the supplier's name in parentheses. The IC_{50} value was measured by the inhibition of S1P-induced cytosolic Ca^{2+} mobilization in CHO cells expressing $S1P_3$ receptor in terms of Fura-2 fluorescence (see Experimental Section). For compounds **9** and **11**, while IC_{50} values were over 20 μM, dose-dependent inhibitions were observed. The asterisk (*) represents the training set for $S1P_3$ receptor antagonists that was used to generate pharmacophore models.

Table 1. Conditions for Pharmacophore Generation along with the Number of Features, with or without the Hydrogen-Bond Acceptor Feature and the Chirality at *C*2 of the (2*R*)- or (2*S*)-Thiazolidine Scaffold in the Training Set

number of features[a]			number of models[b]	
NegI	HBA	HYD	2*R*	2*S*
1	1	1	18	17
1	0	2	15	12
1	1	2	60	49
1	0	3	17	15
1	1	3	52	47
1	0	4	0	5

[a] Number of maximum features used in pharmacophore generation. NegI, negative ionizable feature; HBA, hydrogen-bond acceptor feature; HYD, hydrophobic feature. [b] Number of models generated by using a training set that included (2*R*)- or (2*S*)-thiazolidine-4-carboxylic acid derivatives.

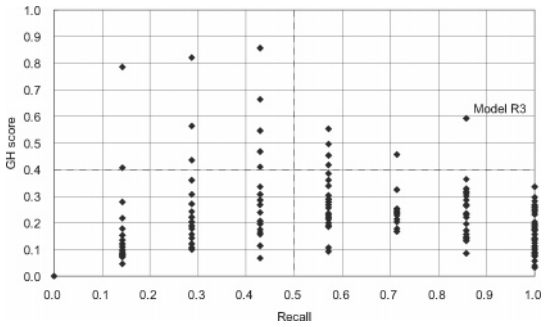

Figure 3. Scatter-diagram analysis of pharmacophore model validations based on the GH score and recall of active compounds. A GH score of 1 means the best (ideal) model and 0 means the worst (null) model. Recall means the yield of known active compounds registered in a database (also called yield of actives (*% Y*)). For example, if a pharmacophore model identifies all seven known actives **6**−**12** as hits among 107 compounds, the recall value is 1 (100%).

showed that the $S1P_3$ antagonist activity of thiazolidine-4-carboxylic acid was increased by lengthening the side alkyl chain at the 2-position up to 11 methylenic groups and then decreased as the number of methylenic groups increased further.[36] One possible explanation for this observation is based on the steric effects of the methyl group C13 in 2-tridecyl thiazolidine-4-carboxylic acid **13** (Figure 5). All seven models in Figure 4 identified **13** as an active compound due to the lack of information about steric properties. Therefore, these models should be improved to take into account steric properties and then further validated.

Overlap between the pharmacophore model and **13** could reveal the 3D-coordinates of C13 positions which are expected as excluded volumes. For that purpose, the following methods were used: (A) All of the generated conformations of **13** with the (2*R*)- or (2*S*)-isomer were superimposed on each pharmacophore model derived from the training set consisting of (2*R*)- or (2*S*)-derivatives, respectively. All of the 3D-coordinates of C13 of **13** were transferred to the center coordinates of excluded volumes (spheres) with radius 1.5 Å and merged with the pharmacophore model. (B) All active compounds **6**−**12** were aligned with each pharmacophore model with the excluded volumes. If an excluded volume sphere partially overlapped any sphere of an atom in active compounds with radius 1.5 Å, this excluded volume was discarded. Consequently, excluded volumes outside the active space were retained. For example, in model R3, 95 excluded volumes surrounding the active space were retained (Figure 6a). (C) Each excluded volume was assessed by the GH score using the above-mentioned database. Only excluded volumes that improved the GH score were retained, since they could filter out inactive compounds, probably based on steric effects. For example, in model R3, three of the 95 excluded volumes were assigned to be associated with steric interaction based on improvement of the GH score (Figure 6b,c).

(iv) Determination of the Most Relevant Pharmacophore Model. As an $S1P_3$ antagonist pharmacophore model, model R3 with three excluded volumes (R3 Ex) was chosen among seven models with excluded volumes based on the GH score (Table 2).

The GH score of model R3 without an excluded volume was 0.59, which was the best among the seven models, and with three excluded volumes this value increased to 0.93, which was also the best among the seven models with excluded volumes. In addition, model R3 could identify both **7** and **9** in the test set that were not used for pharmacophore generation.

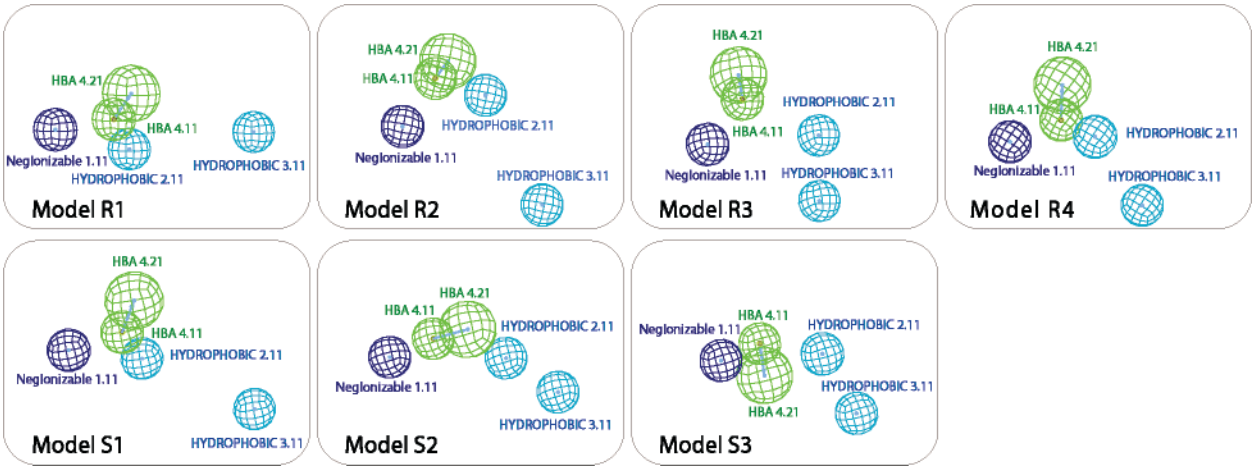

Figure 4. Seven pharmacophore models that consisted of one *negative ionizable*, one *hydrogen-bond acceptor*, and two *hydrophobic* features fulfilled the criteria. The letters R and S with each name indicate the pharmacophore model generated by a training set consisting of (2*R*)- and (2*S*)-thiazolidine derivatives, respectively. Four features: NegIonizable (*negative ionizable*), HYDROPHOBIC (*hydrophobic*) 2.11 and 3.11, and HBA (*hydrogen-bond acceptor*) 4.11 features are represented as spheres with radius 1.72 Å. The HBA (*hydrogen-bond acceptor*) 4.21 feature is the projected point of HBA 4.11 and is represented as a sphere with radius 2.32 Å.

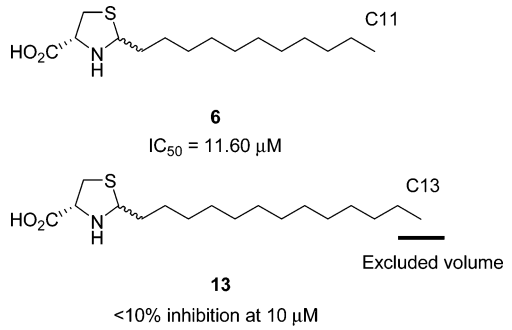

Figure 5. Assumed steric repulsion between $S1P_3$ receptor and **13**. As a possible explanation for the significant decrease in the potency of **13** compared to **6**, steric repulsion with the $S1P_3$ receptor can be approximated at C13 of **13**. In a pharmacophore model, a kind of steric repulsion can be represented by the strategic placement of excluded volume (a sphere that cannot be penetrated by the ligand).

2. Database Searches To Identify $S1P_3$ Receptor Antagonists, Biological Assay, and Results. Model R3 Ex was used to search databases consisting of commercially available compounds. Among the hit list, 36 compounds were selected, purchased, and assayed to identify $S1P_3$ antagonist activity (the structures of all assayed compounds are shown in the Supporting Information).

Among the screened compounds, isophthalic acid derivatives **14**, **15**, and **16** were identified as antagonists for $S1P_3$ receptor (Figure 7). While they showed similar potencies, we chose isophthalic acid derivative **14** for further studies to clarify the structural requirements because it contained fewer carboxylic acids than **15** and **16**. Isophthalic acid **14** was aligned to model R3 Ex (Figure 8a). One of the carboxylic acids on the phenyl ring was recognized as a *negative ionizable* feature. The other carboxylic acid was assumed to act as the *hydrogen-bond acceptor* feature. The 3-methoxyphenyl group, but not the 4-cetyloxy group, was mapped as a *hydrophobic* feature. The direction of the 4-cetyloxy group was different from that of the *m*-substituted alkyl chain in **8** (Figure 8a,b). The piperidine group, which was recognized as a *hydrophobic* feature, was also considered to play an important role in regulating the active conformation.

3. Synthesis of Derivatives and Identification of the Structure−Activity Relationship in an $S1P_3$ Receptor Antagonist. To clarify the minimum structural requirements for **14** as an $S1P_3$ receptor antagonist, derivatives of **14** were synthesized (Scheme 1). We replaced the piperidine group with a phenyl group to simplify synthesis, since we assumed that it acted as a *hydrophobic* feature.

Compound **19** or **20** was coupled with the benzophenone derivative to elucidate whether two carboxylic acids were essential, as the model predicted. Five benzophenone building blocks **21**−**24** were synthesized to clarify the substituent effects of 4-cetyloxy and 3-methoxy groups on the phenyl ring. Both geometric isomers (*E* and *Z* isomers) with regard to the hydrazone moiety were obtained by a coupling reaction. They were purified separately as single isomers by column chromatography. The geometry of the hydrazone bond was assigned by comparison of the ^{13}C NMR chemical shift of the hydrazone carbon of the *E* and *Z* isomers. A steric compression shift that results in an upfield shift is observed in sterically hindered *Z* isomer of oxime or hydrazone by ^{13}C NMR spectroscopy[43−46] and has been used in the studies of diverse organic compounds.[47−50] For example, the ^{13}C NMR chemical shift of the hydrazone carbon of *E* isomer **25E** was 150.04 ppm and that of *Z* isomer **25Z** was 149.26 ppm. Thus, a steric compression shift of 0.78 ppm was observed for the *Z* isomer. Compounds **25**−**29** were purified separately as *E* or *Z* isomers. We obtained the corresponding carboxylic acids **30**−**34** by hydrolysis.

$S1P_3$ receptor antagonist activities of these synthesized derivatives **30**−**34** were evaluated (Table 3). Isophthalic acid **14** retrieved from the database showed an IC_{50} value of 3.44 μM, and this also showed moderate antagonist activity for the $S1P_1$ receptor. Synthesized **30E** showed an IC_{50} value of 2.96 μM. We also synthesized a derivative without this phenyl group, corresponding to compound **30E**; however, $S1P_3$ antagonist activity was not observed at all (data not shown). Therefore, this phenyl group was implicated in the interaction with the $S1P_3$ receptor. None of the synthesized sulfohydrazone derivatives showed more than 50% inhibitory activity for the $S1P_2$ receptor at 10 μM.

In the assay of **32E**, **31E**, and **30E** with 4, 8, and 16 alkyl chain carbons, respectively, the IC_{50} values for the $S1P_3$ receptor and the $S1P_1$ receptor were found to decrease with a decrease in the length of the alkyl chain. Therefore, the length of the alkyl chain at the 4-position of the phenyl ring was the dominant factor for not only the $S1P_3$ receptor but also $S1P_1$ receptor

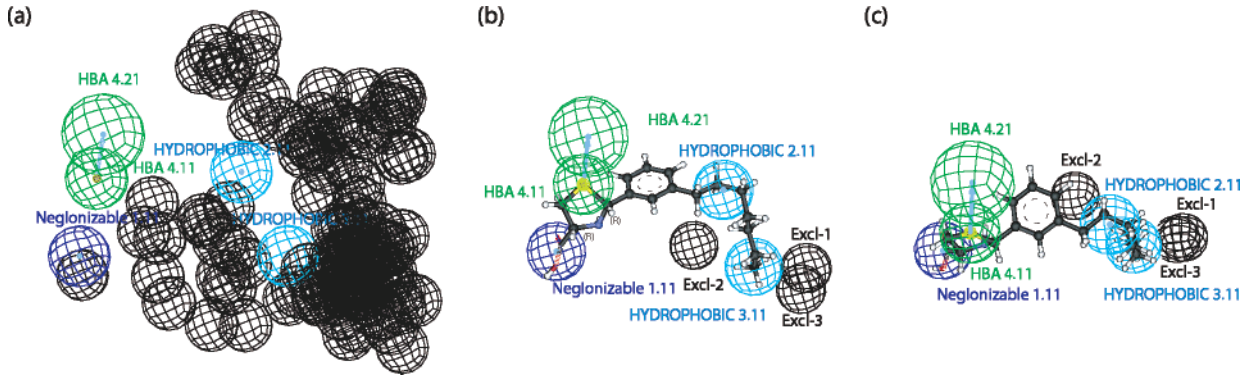

Figure 6. Addition of all excluded volumes to model R3 to identify **13** as inactive. Overlap between the optimized model (R3 Ex) and **8**. (a) Ninety-five 3D coordinates of C13 in compound **13** aligned with model R3 were transferred to the corresponding excluded volumes with radius 1.5 Å and merged into that model. (b and c) Viewpoints of model R3 Ex aligned with compound **8**. Three excluded volumes 1−3 are abbreviated as Excl-1, -2, and -3 and indicated with black mesh.

Table 2. Comparison of Database Searches Using Models R3 and R3 Ex[a]

model	all	actives	hits	tp	fp	tn	fn	%*A*	%*Y*	E	GH
R3	107	7	11	6	5	95	1	54.5	85.7	8.34	0.59
R3 Ex	107	7	5	5	0	100	2	100	71.4	15.3	0.93

[a] All, number of compounds in the database; actives, number of actives in the database; hits, number of hits retrieved by the model (minimum fit value of 90%); tp, number of true positives in the hit list; fp, number of false positives in the hit list; tn, number of true negatives in the hit list; fn, number of false negatives in the hit list.

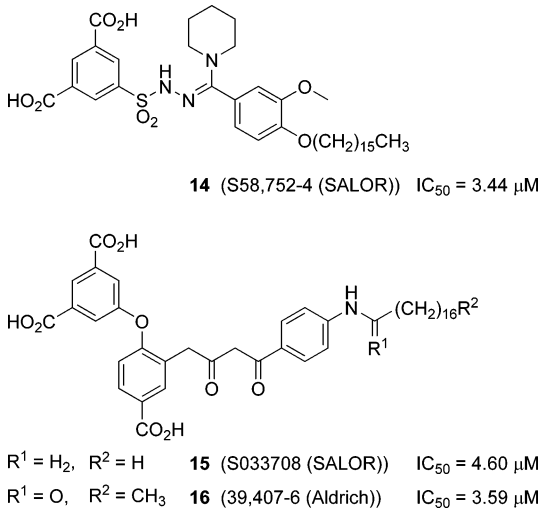

Figure 7. Newly identified $S1P_3$ receptor antagonists obtained via a database search. The supplier's name is given in parentheses. The IC_{50} value was measured by the inhibition of S1P-induced $[Ca^{2+}]_i$ mobilization in CHO cells expressing the $S1P_3$ receptor in terms of Fura-2 fluorescence.

antagonist activity. This tendency was also observed for **31Z** and **30Z**.

As expected based on the pharmacophore model, the carboxylic acid of isophthalic acid, which was identified as a *hydrogen-bond acceptor* feature, was also essential for $S1P_3$ antagonist activity, since benzoic acid derivatives **34E** and **34Z** did not show clear potencies. Compound **30Z** exhibited a similar potency (IC_{50} 3.57 μM) to **30E**. Both of the active conformations **30E** and **30Z** were compared along with model R3 Ex (Figure 9a,b). 3,4-Dialkoxybenzophenone acted as *hydrophobic* 2.11 and 3.11 in both **30E** and **30Z**. The 3-methoxy group of **30E** was superimposed on *hydrophobic* 3.11, as in compound **14**. Meanwhile, the 3-methoxy group of **30Z** could also be superimposed on *hydrophobic* 3.11, since the symmetry of isophthalic acid allowed each carboxylic acid to act as either a *negative ionizable* or *hydrogen-bond acceptor* feature, with the result that **30Z** could be superimposed on the model similar to

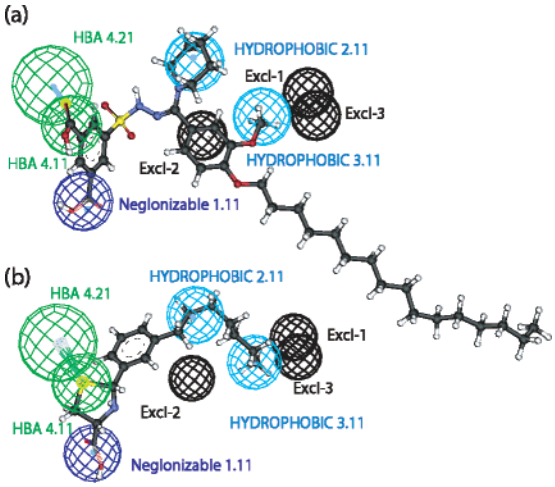

Figure 8. Overlap between model R3 Ex and **14** and **8**. (a) **14** with model R3 Ex. (b) **8** with model R3 Ex.

30E. This assumption regarding the pharmacophore model is consistent with the results of the biological assay. The importance of the 3-methoxy group as the *hydrophobic* feature was supported by the finding that compound **33E**, which does not contain a 3-methoxy group, was less potent than compound **30E**.

As mentioned earlier, the 4-cetyloxy group did not correspond to the meta-substituted alkyl chain of compound **8** (Figure 8a,b). However, the 4-cetyloxy group in isophthalic acid derivatives was significantly associated with antagonist activities for $S1P_1$ and $S1P_3$ receptors. Taken together, these results suggest that the 4-cetyloxy group plays a role corresponding to the alkyl chain of S1P. Initially, we hypothesized that the hydrophobic space represented by *hydrophobic* 2.11 and 3.11 corresponded to the alkyl chain of S1P. However, we now believe that it works differently than S1P and is significantly associated with antagonist activity for the $S1P_3$ receptor. Thus, a 3,4-dialkoxybenzophenone scaffold which fulfilled this hydrophobic space could be a potent component of an $S1P_3$ receptor antagonist. Meanwhile, since a 4-cetyloxy group may play a role similar to that of the alkyl chain of S1P, it is assumed to contribute to

Scheme 1. Synthesis of 5-sulfohydrazono-1,3-isophthalic Acid Derivatives and 3-Sulfohydrazonobenzoic Acid Derivatives[a]

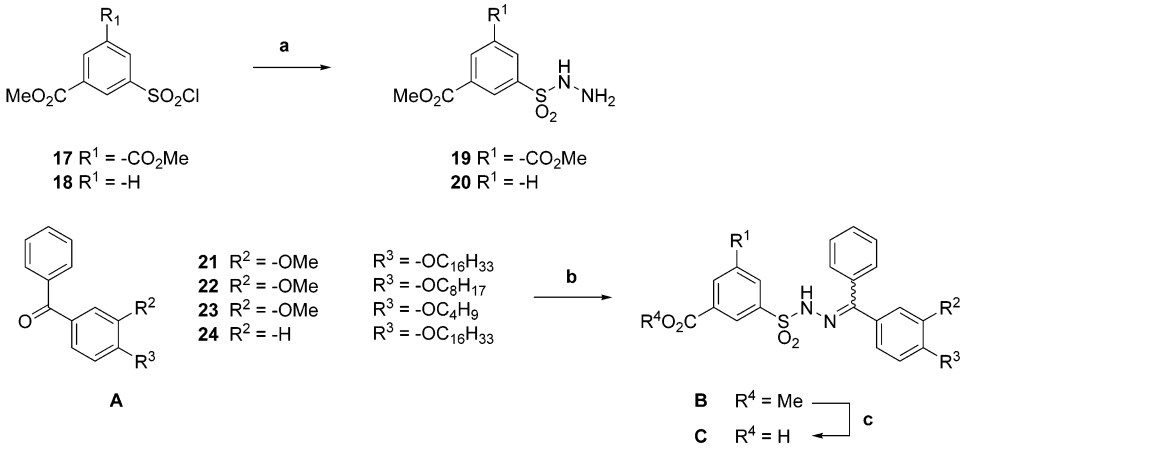

A	B	C	R^1	R^2	R^3	*E*/*Z*	% yield of **B**
21	**25E**	**30E**	-CO_2H	-OMe	-$OC_{16}H_{33}$	*E*	70
	25Z	**30Z**	-CO_2H	-OMe	-$OC_{16}H_{33}$	*Z*	7
22	**26E**	**31E**	-CO_2H	-OMe	-OC_8H_{17}	*E*	70
	26Z	**31Z**	-CO_2H	-OMe	-OC_8H_{17}	*Z*	26
23	**27E**	**32E**	-CO_2H	-OMe	-OC_4H_9	*E*	91
	-	-	-CO_2H	-OMe	-OC_4H_9	*Z*	0
24	**28E**	**33E**	-CO_2H	H	-$OC_{16}H_{33}$	*E*	61
	-	-	-CO_2H	H	-$OC_{16}H_{33}$	*Z*	trace
21	**29E**	**34E**	H	-OMe	-$OC_{16}H_{33}$	*E*	32
	29Z	**34Z**	H	-OMe	-$OC_{16}H_{33}$	*Z*	50

[a] Reagents and conditions: (a) NH_2NH_2·H_2O, THF, 0 °C; (b) **19** or **20**, MeOH, reflux; (c) 1N NaOH, THF−MeOH.

Table 3. $S1P_3$ Receptor Antagonist Activities of Synthesized Isophthalic Acid Derivatives[a]

	IC_{50} (μM)		
compd	$S1P_3$	$S1P_1$	$S1P_2$
14	3.44	6.18	(35.9%)
30E	2.96	6.64	(40.9%)
30Z	3.57	4.28	(9.5%)
31E	11.39	(12.7%)	(−4.6%)
31Z	13.23	(32.9%)	(14.0%)
32E	(6.7%)	(24.2%)	(6.2%)
33E	9.74	(17.2%)	(20.5%)
34E	(34.4%)	(34.8%)	(−0.1%)
34Z	(8.3%)	(1.0%)	(−8.7%)

[a] The IC_{50} value was measured by the inhibition of S1P-induced $[Ca^{2+}]_i$ mobilization in CHO cells expressing $S1P_1$, $S1P_2$, or $S1P_3$ receptor in terms of Fura-2 fluorescence. For a compound with lower potency, for which it was difficult to measure an accurate IC_{50} value, the percent inhibition at 10 μM is given in parentheses.

all S1P receptors and to lack selectivity for $S1P_3$ receptor antagonism. Thus, **31E** with a moderate alkyl chain may be useful not only for exploring a more selective pharmacophore model for $S1P_3$ receptor antagonists but also as a better starting point to obtain a more potent and selective $S1P_3$ receptor antagonist than **14** and **30E**.

4. Assessment of the Model Using Different $S1P_3$ Receptor Antagonists. Although the pharmacophore model identified a potent scaffold, it was based on a training set that consisted of compounds with limited diversity and activities. To generate a feature-based pharmacophore model, structural diversity is important for exploring the key structural features. In addition, there were too few compounds in the test set. Thus, the pharmacophore model was further evaluated using different $S1P_3$

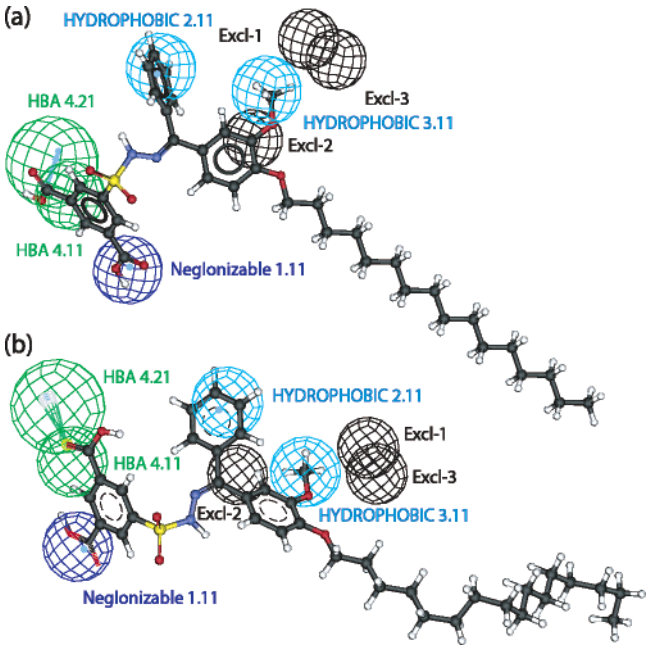

Figure 9. Overlap analysis of *E* and *Z* isomers. (a) **30E** (*E* isomer) with model R3 Ex. (b) **30Z** (*Z* isomer) with model R3 Ex.

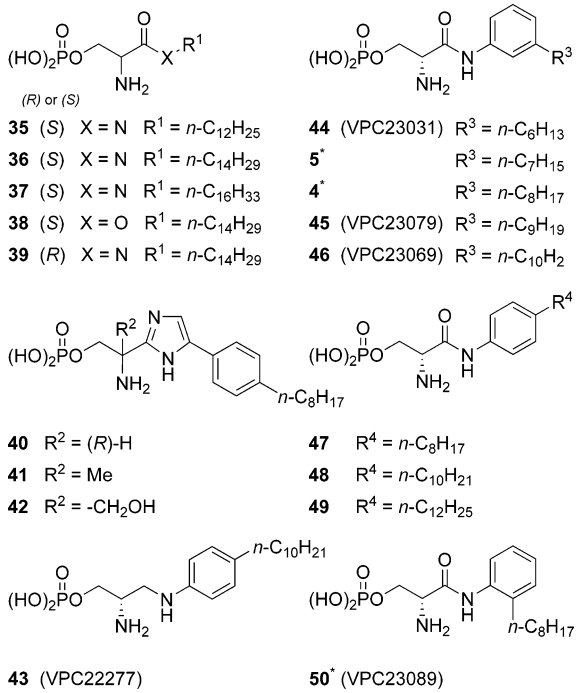

Figure 10. $S1P_1/S1P_3$ receptor agonists and antagonists reported by the University of Virginia. The three asterisks (*) represent the reported $S1P_1/S1P_3$ receptor antagonists, and their antagonist activities for the $S1P_3$ receptor were determined by a [^{32}P]-S1P binding assay (**4**; K_i = 1175 nM, **5**; K_i = 98 nM, **50**; K_i = 1586 nM).[32] Compounds **35**−**42** and **47**−**49** were reported to be $S1P_1/S1P_3$ receptor agonists with EC_{50} values for the $S1P_3$ receptor that were greater than 1000 nM based on a [^{35}S]- γ-GTP binding assay.[51,52] Compounds **43** and **46** were reported to be both $S1P_1$ receptor agonists and $S1P_3$ receptor partial agonist and weak partial agonist, respectively.[32] Compound **44** was reported to be an $S1P_1$ receptor antagonist and **45** was reported as an $S1P_1/S1P_4$ receptor agonist.[32]

receptor antagonists to see whether the model could identify the same key features for $S1P_3$ receptor antagonism in our result.

Recently, researchers at the University of Virginia reported that phosphates **4**, **5**, and **50** were $S1P_1/S1P_3$ receptor antagonists based on the result of [^{35}S]-γ-GTP binding and [^{32}P]-S1P binding assays (Figure 10).[32] Meanwhile, most of the derivatives in Figure 10 were reported to act as $S1P_3$ receptor agonists.[32,51,52] They were useful for assessing the potency of the pharmacophore model for $S1P_3$ receptor antagonists, since they included agonists (**35**−**43** and **46**−**49**), antagonists (**4**, **5**, and **50**) and inactive compounds (**44** and **45**) for the $S1P_3$ receptor. Model R3 Ex was applied to elucidate if it could efficiently identify the antagonists among them.

As a result, model R3 Ex identified only **5** as an active compound among the 18 derivatives in Figure 10. Although **4** and **50** were reported to be $S1P_3$ receptor antagonists, their K_i values were less than one-tenth that of **5**. Thus, the results based on the pharmacophore model are consistent with the reported $S1P_3$ receptor antagonist actives. The terminal alkyl group of the C7 alkyl chain in **5** was superimposed on *hydrophobic* 3.11, as in **8** (Figure 11a). Meanwhile, **44**, with a C6 alkyl chain, which was reported to not act as an $S1P_3$ receptor agonist or antagonist, had an alkyl chain that was too short to reach *hydrophobic* 3.11 (Figure 11b) and thus showed a lower fit value than **5**. In addition, since **4** with a C8 alkyl chain, which is one carbon longer than that in **5**, also shows a lower fit value than **5**, it may have reduced the potency due to repulsion between excluded volumes.

The potency for $S1P_3$ receptor antagonism was reported to differ significantly among **44**, **5**, and **4** with C6, C7, and C8

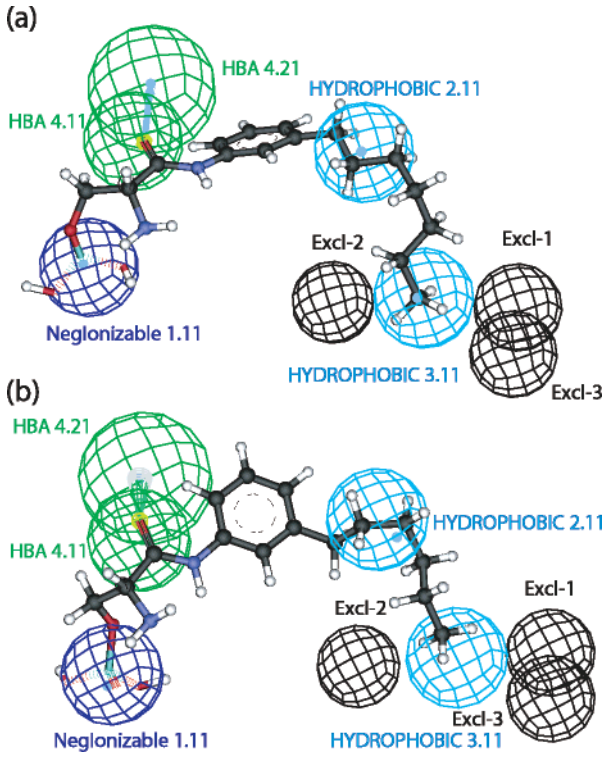

Figure 11. Overlap between model R3 Ex and **5** with a C7 alkyl chain and **44** with a C6 alkyl chain. (a) **5** with model R3 Ex. (b) **44** with model R3 Ex. Since **5** with model R3 Ex shows a better fit than **44**, the terminal alkyl group of the C7 alkyl chain in **5** is assumed to be important for $S1P_3$ receptor antagonism. This perspective is consistent with their reported K_i values.

alkyl chains, respectively.[32] As mentioned, the pharmacophore model provided one possible explanation for the sensitivity of these antagonist activities for the $S1P_3$ receptor. This perspective is consistent with our results. In addition, the antagonist activities of these compounds for the $S1P_1$ receptor were reported to not be influenced by the length of their alkyl chains.[32] If we consider all of these results, while the pharmacophore model has not clarified the role of *hydrogen-bond acceptor* feature, at least the hydrophobic space including *hydrophobic* 2.11 and 3.11 features surrounded by excluded volumes is assumed to play the key important role for $S1P_3$ receptor antagonism.

Conclusion

Our results demonstrate that a pharmacophore model constructed by common feature-based alignment can be used for scaffold-hopping to efficiently identify diverse active compounds prior to biological testing. For that purpose, the GH score based on well-selected structures was useful as a metric for determining relevant excluded volumes and obtaining a reliable pharmacophore model. Isophthalic acid derivatives were identified as novel and potent $S1P_3$ receptor antagonists by a pharmacophore-based database search. On the basis of a consideration of structure−activity relationships, the 3,4-dialkoxybenzophenone scaffold was found to be a potent component of an $S1P_3$ receptor antagonist. The key feature for $S1P_3$ receptor antagonism which was described by *hydrophobic* features with excluded volumes was assumed to be different from the space occupied by the alkyl chain of S1P. Further studies are underway to identify selective $S1P_3$ receptor antagonists by pharmacophore-based design.

Experimental Section

Pharmacophore Modeling Studies. Pharmacophore models were generated with the HipHop module of Catalyst 4.9[38,53] on an Intel-based PC running the Red Hat Enterprise Linux WS 3.0 operating system. Conformational models of all compounds were calculated using an energy cutoff of 15 kcal in Best mode. The number of conformers generated for each molecule was limited to a maximum of 255. Pharmacophore generation was conducted by the feature-based alignment of five active compounds: **6**, **8**, **10**, **11**, and **12**. Compound **8** was used as the central compound to generate pharmacophore models. The database used for GH score-based validation was constructed using Catalyst/catDB, and the maximum number of conformers per compound was set at 255 in Best mode.

Conformers of (2*R*)- and (2*S*)-**13** were generated with the above-mentioned conditions and 182 and 204 conformers were obtained, respectively. All conformations in (2*R*)- or (2*S*)-**13** were aligned with the pharmacophore model derived from the training set consisting of (2*R*)- or (2*S*)-derivatives, respectively. All superimposed 3D-coordinates of C13 of **13** in the pharmacophore models were exported using the Catalyst/citest command and converted into the excluded volumes (spheres) with radius 1.5 Å. The seven active compounds of the training set were also aligned with the pharmacophore models, and the 3D-coordinates of all atoms were exported using the Catalyst/citest command and converted into atom spheres with radius 1.5 Å. Excluded volumes that overlapped any atom sphere with radius 1.5 Å were omitted because of inappropriate 3D-coordinates for an excluded volume. Appropriate excluded volumes that improved the GH score were identified and incorporated into the pharmacophore model. The Minimum Fit for Search option of the pharmacophore model was set at 3.6, which was 90% of the maximum fit value. A database search was conducted with a fast flexible search.

Stable Expression of S1P Receptors in CHO-K1 Cells. CHO-K1 cells (Dainippon Sumitomo Pharma) were transfected using Lipofectamine 2000 (Invitrogen) with pcDNA3.1 (+) plasmid (Sigma-Aldrich) encoding the human $S1P_1$ or $S1P_3$ receptor and neomycin (G418) resistance or pFLAG-CMV9 plasmid (Sigma-Aldrich) encoding the human $S1P_2$ receptor and G418 resistance. Cells were grown in Ham's F12K medium supplemented with G418 (200 μg/mL, Sigma-Aldrich).

Measurement of Intracellular Calcium Mobilization. A FlexStation II fluorimeter (Molecular Devices) was used to measure the intracellular calcium concentration ($[Ca^{2+}]_i$) in CHO-K1 cells that had been stably transfected with $S1P_1$, $S1P_2$, or $S1P_3$ receptors. Suspensions of cells in a nutrient mixture of Ham's medium containing 1% (v/v) fetal bovine serum (FBS) were loaded (20 000 cells/well) in 96-well, clear-bottom black microplates (Greiner Bio-One) and left for 24 h at 37 °C. The cells were washed and then incubated in Ham's medium for 24 h at 37 °C.

Cells were washed and dye-loaded with Fura2-AM ester (5 μM, Molecular Probes) in Hanks balanced salt solution (HBSS) containing sulfinpyrazone (0.25 mmol/l, Sigma-Aldrich) for 60 min at 37 °C. After cell monolayers were washed with HBSS containing sulfinpyrazone (0.25 mmol/L), loading buffer was added, and cells were exposed to the test compound for 5 min. After S1P was added (10 nmol, Sigma-Aldrich), fluorescence (excitation at 335 and 362 nm; emission at 505 and 512 nm) was immediately measured for 45 s at intervals of 3 s with a FlexStation II. A curve-fitting algorithm (Model 08: Sigmoidal Inhibition Curve) implemented in MDL Assay Explorer[54] was used to calculate the IC_{50} value.

Chemistry. General Information. Melting points were determined with a Yanako MP-500V micro melting point apparatus (uncorrected), and ^{1}H and ^{13}C NMR spectra were recorded on a JEOL JNM-AL-300, using $CDCl_3$ or DMSO-d_6 as solvents, with Me_4Si as an internal standard. Mass spectra were recorded on either a JEOL HX-110A (FAB) or Finnigan LCQ (ESI). Elemental analysis (C, H, N) was performed on a Carloerba EA-1108 at Tokyo Chemical Industry Co., Ltd. Reactions were monitored by TLC analysis using E. Merck silica gel $60F_{254}$ thin layer plates. Flash chromatography was carried out on E. Merck Kieselgel 60 (230−400 mesh) silica gel.

5-Chlorosulfonyl Isophthalic Acid Dimethyl Ester (17). To a suspension of dimethyl 5-sulfoisophthalate sodium salt (5.70 g, 19.24 mmol) in CCl_4 (250 mL) were added PCl_5 (20.23 g, 96.21 mmol) and diisopropylamine (2.5 mL, 17.66 mmol). The mixture was refluxed for 6 h, diluted with H_2O at 0 °C, extracted with $CHCl_3$, washed sequentially with H_2O and brine, dried over Na_2SO_4, filtered, and concentrated. Recrystallization from diethylether/hexane gave **17** as a colorless powder (3.16 g, 56%). mp 91−92 °C; ^{1}H NMR (300 MHz, $CDCl_3$) δ 9.00 (s, 1H), 8.85 (s, 2H), 4.03 (s, 6H); ^{13}C NMR (75 MHz, $CDCl_3$) δ 163.88, 145.13, 136.48, 132.66, 131.57, 53.19; MS (FAB) *m*/*z* 292 (M^+); Anal. ($C_{10}H_9ClO_6S$) calcd, C 41.04; H 3.10; found, C 41.35, H 3.10.

5-Hydrazosulfonyl Benzene-1,3-Carboxylic Acid Dimethyl Ester (19). A solution of hydrazine hydrate (3.28 g, 65.60 mmol) in EtOH (50 mL) was added to a stirred **17** (3.84 g, 13.12 mmol) in $CHCl_3$ (100 mL). The mixture was stirred for 6 h, diluted with $CHCl_3$, washed sequentially with H_2O and brine, dried over Na_2SO_4, filtered, and concentrated. Recrystallization from diethylether/hexane gave **19** as colorless needles (2.11 g, 56%). mp 142−143 °C; ^{1}H NMR (300 MHz, $CDCl_3$) δ 8.91 (s, 1H), 8.73 (d, J = 1.65 Hz, 2H), 4.00 (s, 6H); ^{13}C NMR (75 MHz, $CDCl_3$) δ 164.56, 139.10, 135.04, 132.95, 132.09, 52.98; MS (FAB) *m*/*z* 288 (M^+); Anal. ($C_{10}H_{12}N_2O_6S$) calcd, C 41.66; H 4.20; N, 9.72; found, C, 41.72; H, 4.09; N, 9.55.

3-Methoxycarbonylbenzenesufohydrazide (20). A suspension of 5-chlorosulfonylbenzoic acid (1.10 g, 5.00 mmol) in thionyl chloride (5 mL) was refluxed for 2 h. The mixture was concentrated, dissolved in methanol (10 mL), stirred for 15 min, and concentrated. The residue of **18** was dissolved in THF (10 mL). To the solution was added hydrazine hydrate (0.36 mL, 7.50 mmol). The mixture was stirred for 30 min at 0 °C, diluted with $CHCl_3$, washed sequentially with H_2O and brine, dried over Na_2SO_4, filtered, and concentrated. Recrystallization from chloroform/diethylether gave **20** as a colorless powder (367 mg, 32%). mp 87−89 °C; ^{1}H NMR (300 MHz, $CDCl_3$) δ 8.55 (brs, 1H), 8.33 (s, 1H), 8.19 (d, J = 7.71 Hz, 1H), 8.04 (d, J = 7.94 Hz, 1H), 7.76 (dd, J = 7.94, 7.71 Hz, 1H), 4.21(brs, 2H), 3.90 (s, 3H); ^{13}C NMR (75 MHz, $CDCl_3$) δ 165.36, 137.19, 134.30, 132.23, 131.41, 129.57, 129.21, 52.70; MS (FAB) *m*/*z* 230 (M^+); Anal. ($C_8H_{10}N_2O_4S$) calcd, C, 41.73; H, 4.38; N, 12.17; found, C, 42.08; H, 4.26; N, 11.95.

4-Cetyloxy-3-methoxybenzophenone (21). To a solution of 4-hydroxy-3-methoxybenzophenone[55] (342 mg, 1.50 mmol) in DMF (10 mL) were added sodium carbonate (249 mg, 1.80 mmol) and cetyl bromide (0.69 mL, 2.25 mmol). The mixture was stirred for 2 h at 80 °C, diluted with ethyl acetate, washed sequentially with H_2O and brine, dried over Na_2SO_4, filtered, and concentrated. Column chromatography (10:1 hexane:ethyl acetate) provided **21** as a colorless powder (605 mg, 89%). mp 57−58 °C; ^{1}H NMR (300 MHz, $CDCl_3$) δ 7.75 (dd, J = 8.63, 1.65 Hz, 2H), 7.59−7.54 (m, 1H), 7.50−7.45 (m, 3H), 7.36 (dd, J = 8.42, 2.01 Hz, 1H), 6.88 (d, J = 8.42 Hz, 1H), 4.09 (t, J = 7.03 Hz, 2H), 3.93 (s, 3H), 1.89 (dt, J = 7.03, 6.89 Hz, 2H), 1.49−1.42 (m, 2H), 1.38−1.22 (m, 24H), 0.88 (t, J = 6.61 Hz, 3H); ^{13}C NMR (75 MHz, $CDCl_3$) δ 195.64, 152.70, 149.21, 138.37, 131.81, 129.87, 129.72, 128.15, 125.53, 112.40, 110.76, 69.09, 56.11, 31.93, 29.69, 29.66, 29.60, 29.55, 29.37, 28.96, 25.91, 22.70, 14.13; MS (FAB) *m*/*z* 452 (M^+); Anal. ($C_{30}H_{44}O_3$) calcd, C, 79.60; H, 9.80; found, C, 79.35; H, 10.0.

4-Octyloxy-3-methoxybenzophenone (22). Compound **22** was prepared according to the procedure described for **21** but with octyl bromide instead of cetyl bromide. Compound **22** was obtained as a colorless powder (604 mg, quant). mp 34−35 °C; ^{1}H NMR (300 MHz, $CDCl_3$) δ 7.76 (dd, J = 8.44, 1.47 Hz, 2H), 7.59−7.54 (m, 1H), 7.50−7.45 (m, 3H), 7.36 (dd, J = 8.44, 2.02 Hz, 1H), 6.88 (d, J = 8.44 Hz, 1H), 4.09 (t, J = 6.97 Hz, 2H), 3.93 (s, 3H), 1.87 (dt, J = 6.97, 6.79 Hz, 2H), 1.49−1.46 (m, 2H), 1.33−1.23 (m, 8H), 0.89 (t, J = 6.97 Hz, 3H); ^{13}C NMR (75 MHz, $CDCl_3$) δ 195.38, 152.61, 149.12, 138.24, 131.65, 129.76, 129.56, 128.00, 125.37, 112.32, 110.70, 68.94, 55.94, 31.66, 29.20, 29.07, 28.86,

25.79, 22.52, 13.97; MS (FAB) *m*/*z* 340 (M^+); Anal. ($C_{22}H_{28}O_3$) calcd, C, 77.61; H, 8.29; found, C, 77.39; H, 8.41.

4-Butyloxy-3-methoxybenzophenone (23). Compound **23** was prepared according to the procedure described for **21** but with butyl bromide instead of cetyl bromide. Compound **23** was obtained as a colorless powder (435 mg, 87%). mp 75−76 °C; ^{1}H NMR (300 MHz, $CDCl_3$) δ 7.77 (dd, J = 8.26, 1.29 Hz, 2H), 7.59−7.54 (m, 1H), 7.50−7.45 (m, 3H), 7.36 (dd, J = 8.26, 2.02 Hz, 1H), 6.88 (d, J = 8.26 Hz, 1H), 4.10 (t, J = 6.79 Hz, 2H), 3.92 (s, 3H), 1.86 (dt, J = 7.52, 6.79 Hz, 2H), 1.56−1.48 (m, 2H), 0.99 (t, J = 7.34 Hz, 3H); ^{13}C NMR (75 MHz, $CDCl_3$) δ 195.52, 152.69, 149.19, 138.31, 131.73, 129.85, 129.64, 128.08, 125.44, 112.42, 110.77, 68.70, 56.05, 30.96, 19.11, 13.78; MS (FAB) *m*/*z* 284 (M^+); Anal. ($C_{18}H_{20}O_3$) calcd, C, 76.03; H, 7.09; found, C, 75.97; H, 7.18.

4-Cetyloxybenzophenone (24). Compound **24** was prepared according to the procedure described for **21** but with 4-hydroxybenzophenone instead of 4-hydroxy-3-methoxybenzophenone. Compound **24** was obtained as a colorless powder (1.14 g, 90%). mp 66−67 °C; ^{1}H NMR (300 MHz, $CDCl_3$) δ 7.82 (d, J = 8.84 Hz, 2H), 7.75 (dd, J = 8.44, 1.46 Hz, 2H), 7.59−7.53 (m, 1H), 7.49−7.44 (m, 2H), 6.95 (d, J = 8.84 Hz, 2H), 4.03 (t, J = 6.61 Hz, 2H), 1.82 (dt, J = 6.90, 6.61 Hz, 2H), 1.52−1.22 (m, 26H), 0.88 (t, J = 6.61 Hz, 3H); ^{13}C NMR (75 MHz, $CDCl_3$) δ 195.57, 162.84, 138.29, 132.55, 131.81, 129.80, 129.70, 128.13, 113.94, 68.24, 31.90, 29.68, 29.64, 29.58, 29.54, 29.35, 29.08, 25.96, 22.68, 14.12; MS (FAB) *m*/*z* 422 (M^+); Anal. ($C_{29}H_{42}O_2$) calcd, C, 82.41; H, 10.02; found, C, 82.55; H, 10.08.

4-Cetyloxy-3-methoxybenzophenone (*E*)-3,5-dimethoxycarbonylphenylsulfohydrazone (25E) and **4-Cetyloxy-3-methoxybenzophenone (*Z*)-3,5-dimethoxycarbonylphenylsulfohydrazone (25Z).** To a solution of **19** (562 mg, 1.95 mmol) in methanol (13 mL) was added **21** (588 mg, 1.30 mmol). The mixture was refluxed for 18 h, diluted with $CHCl_3$, washed with 1 N hydrochloric acid and brine, dried over Na_2SO_4, filtered, and concentrated. Column chromatography (5:1 hexane:ethyl acetate) provided **25E** as a colorless powder (656 mg, 70%) and **25Z** as a colorless powder (64 mg, 7%). Compound **25E**: mp 124−126 °C; ^{1}H NMR ($CDCl_3$) δ 8.89 (t, J = 1.55 Hz, 1H), 8.84(d, J = 1.65 Hz, 2H), 7.77 (brs, 1H), 7.49 (dd, J = 8.08, 1.65 Hz, 2H), 7.38−7.29 (m, 3H), 6.97 (d, J = 8.11 Hz, 1H), 6.71 (dd, J = 8.11, 1.80 Hz, 1H), 6.60 (d, J = 1.80 Hz, 1H), 4.08 (t, J = 7.02 Hz, 2H), 4.00 (s, 6H), 3.80 (s, 3H), 1.89 (dt, J = 7.02, 6.89 Hz, 2H), 1.52−1.22 (m, 26H), 0.88 (t, J = 6.21 Hz, 3H); ^{13}C NMR ($CDCl_3$) δ 164.63, 155.34, 150.17, 150.04, 139.78, 136. 27, 134.77, 132.78, 131.80, 130.11, 128.21, 127.84, 122.27, 121.09, 112.93, 111.16, 69.06, 56.10, 52.87, 31.89, 29.67, 29.59, 29.55, 29.37, 29.34, 29.00, 25.93, 22.66, 14.12; MS (ESI) *m*/*z* 722 (M^+); Anal. ($C_{40}H_{54}N_2O_8S$) calcd, C, 66.46; H, 7.53; N, 3.87; found, C, 66.45; H, 7.53; N, 3.89. Compound **25Z**: mp 73−74 °C; ^{1}H NMR ($CDCl_3$) δ 8.88 (t, J = 1.65 Hz, 1H), 8.82 (d, J = 1.65 Hz, 2H), 8.54 (brs, 1H), 7.54−7.49 (m, 3H), 7.33 (d, J = 1.71 Hz, 1H), 7.14−7.11 (m, 2H), 6.67 (d, J = 8.43 Hz, 1H), 6.61 (dd, J = 8.43, 1.71 Hz, 1H), 3.99 (t, J = 6.80 Hz, 2H), 3.98 (s, 6H), 3.87 (s, 3H), 1.81 (dt, J = 7.21, 6.80 Hz, 2H), 1.44−1.22 (m, 26H), 0.88 (t, J = 6.43 Hz, 3H); ^{13}C NMR ($CDCl_3$) δ 164.64, 155.33, 150.76, 149.26, 139.93, 134.76, 132.86, 131.86, 130.92, 130.23, 129.77, 128.61, 128.25, 122.31, 111.25, 109.22, 68.94, 55.94, 52.87, 31.93, 29.69, 29.65, 29.59, 29.53, 29.36, 28.98, 25.90, 22.70, 14.13; MS (ESI) *m*/*z* 722 (M^+); Anal. ($C_{40}H_{54}N_2O_8S$) calcd, C, 66.46; H, 7.53; N, 3.87; found, C, 66.34; H, 7.56; N, 3.90.

4-Octyloxy-3-methoxybenzophenone (*E*)-3,5-Dimethoxycarbonylphenylsulfohydrazone (26E) and 4-Octyloxy-3-methoxybenzophenone (*Z*)-3,5-dimethoxycarbonylphenylsulfohydrazone (26Z). Compounds **26E** and **26Z** were prepared according to the procedure described for **25E** and **25Z** but with **22** instead of **21**. Compound **26E** was obtained as a colorless powder (500 mg, 72%), and **26Z** was obtained as a colorless powder (187 mg, 27%). Compound **26E**: mp 136−137 °C; ^{1}H NMR (300 MHz, $CDCl_3$) δ 8.89 (t, J = 1.47 Hz, 1H), 8.84 (d, J = 1.47 Hz, 2H), 7.76 (brs, 1H), 7.48 (d, J = 8.44 Hz, 2H), 7.36−7.29 (m, 3H), 6.98 (d, J = 8.26 Hz, 1H), 6.71 (dd, J = 8.26, 2.02 Hz, 1H), 6.61 (d, J = 2.02 Hz, 1H), 4.08 (t, J = 6.97 Hz, 2H), 4.00 (s, 6H), 3.80 (s, 3H), 1.88 (dt, J = 7.89, 6.97 Hz, 2H), 1.51−1.47 (m, 2H), 1.35−1.30 (m, 8H), 0.89 (t, J = 6.79 Hz, 3H); ^{13}C NMR (75 MHz, $CDCl_3$) δ 164.68, 155.37, 150.29, 150,09, 139.85, 136.32, 134.81, 132.81, 131.87, 130.14, 128.25, 127.89, 122.34, 121.13, 113.07, 111.27, 69.13, 56.17, 52.89, 31.82, 29.34, 29.23, 29.04, 25.98, 22.66, 14.12; MS (ESI) *m*/*z* 610 (M^+); Anal. ($C_{32}H_{38}N_2O_8S$) calcd, C, 62.93; H, 6.27; N, 4.59; found, C, 62.93; H, 6.26; N, 4.61. Compound **26Z**: mp 110−111 °C; ^{1}H NMR (300 MHz, $CDCl_3$) δ 8.88 (d, J = 1.65 Hz, 1H), 8.84−8.82 (m, 2H), 7.54−7.52 (m, 3H), 7.33 (d, J = 1.65 Hz, 1H), 7.15−7.12 (m, 2H), 6.69−6.63 (m, 2H), 4.00−3.95 (m, 8H), 3.87 (s, 3H), 1.85−1.79 (m, 2H), 1.49−1.45 (m, 2H), 1.39−1.24 (m, 8H), 0.87 (t, J = 6.97 Hz, 3H); ^{13}C NMR (75 MHz, $CDCl_3$) δ 164.62, 155.31, 150.71, 149.25, 139.90, 134.74, 132.84, 131.83, 130.89, 130.20, 129.75, 128.58, 128.22, 122.30, 111.22, 109.17, 68.91, 55.91, 52.85, 31.75, 29.29, 29.16, 28.93, 25.86, 22.61, 14.08; MS (ESI) *m*/*z* 610 (M^+); Anal. ($C_{32}H_{38}N_2O_8S$) calcd, C, 62.93; H, 6.27; N, 4.59; found, C, 62.64; H, 6.10; N, 4.40.

4-Butylloxy-3-methoxybenzophenone (*E*)-3,5-Dimethoxycarbonylphenylsulfohydrazone (27E). Compound **27E** was prepared according to the procedure described for **25E** and **25Z** but with **23** instead of **21**. Compound **27E** was obtained as a colorless powder (760 mg, 91%). mp 179−181 °C; ^{1}H NMR (300 MHz, $CDCl_3$) δ 8.89 (t, J = 1.47 Hz, 1H), 8.84 (d, J = 1.47 Hz, 2H), 7.78 (s, 1H), 7.48 (dd, J = 8.44, 1.65 Hz, 2H), 7.36−7.29 (m, 3H), 6.98 (d, J = 8.26 Hz, 1H), 6.71 (dd, J = 8.26, 2.02 Hz, 1H), 6.61 (d, J = 2.02 Hz, 1H), 4.09 (t, J = 6.79 Hz, 2H), 4.00 (s, 6H), 3.80 (s, 3H), 1.88 (dt, J = 7.16, 6.79 Hz, 2H), 1.58−1.50 (m, 2H), 1.01 (t, J = 7.34 Hz, 3H); ^{13}C NMR (75 MHz, $CDCl_3$) δ 164.68, 155.36, 150.25, 139.81, 136.29, 134.82, 132.81, 131.85, 130.15, 128.25, 127.88, 122.29, 121.11, 114.00, 113.00, 111.22, 68.75, 56.15, 52.90, 31.05, 19.21, 13.86; MS (ESI) *m*/*z* 554 (M^+); Anal. ($C_{28}H_{30}N2O_8S$) calcd, C, 60.64; H, 5.45; N, 5.05; found, C, 60.74; H, 5.34; N, 5.27.

4-Cetyloxybenzophenone (*E*)-3,5-dimethoxycarbonylphenylsulfohydrazone (28E). Compound **28E** was prepared according to the procedure described for **25E** and **25Z** but with **24** instead of **21**. Compound **28E** was obtained as a colorless powder (84 mg, 61%). mp 141−143 °C; ^{1}H NMR (300 MHz, $CDCl_3$) δ 8.89 (t, J = 1.48 Hz, 1H), 8.83 (d, J = 1.48 Hz, 2H), 7.45 (d, J = 7.17 Hz, 2H), 7.36−7.28 (m, 4H), 7.10 (d, J = 8.62 Hz. 2H), 7.01 (d, J = 8.62 Hz, 2H), 4.02 (t, J = 6.41 Hz, 2H), 4.00 (s, 6H), 1.83 (dt, J = 7.01, 6.41 Hz, 2H), 1.24−1.51 (m, 26H), 0.88 (t, J = 6.63 Hz, 3H); ^{13}C NMR (75 MHz, $CDCl_3$) δ 164.68 160.56, 139.82, 136.51, 134.82, 132.83, 131.86, 130.11, 130.00, 128.22, 127.93, 122.13, 115.61, 68.27, 52.88, 31.93, 29.70, 29.60, 29.36, 29.15, 26.04, 22.70, 14.13; MS (ESI) *m*/*z* 692 (M^+); Anal. ($C_{39}H_{52}N_2O_7S$) calcd, C, 67.60; H, 7.56; N, 4.04; found, C, 67.39; H, 7.62; N, 4.02.

4-Cetyloxy-3-methoxybenzophenone (*E*)-3-Methoxycarbonylphenylsulfohydrazone (29E) and **4-Cetyloxy-3-methoxybenzophenone (*Z*)-3-Methoxycarbonylphenylsulfohydrazone (29Z).** Compounds **29E** and **29Z** were prepared according to the procedure described for **25E** and **25Z**, but with **20** instead of **19**. Compound **29E** was obtained as a colorless powder (84 mg, 32%) and **29Z** was obtained as a colorless powder (132 mg, 50%). Compound **29E**: mp 85−86 °C; ^{1}H NMR (300 MHz, $CDCl_3$) δ 8.66 (dd, J = 1.83, 1.38 Hz, 1H), 8.27(ddd, J = 7.91, 2.93, 1.38 Hz, 1H), 8.19 (ddd, J = 7.83, 2.93, 1.83 Hz, 1H), 7.75 (brs, 1H), 7.65 (dd, J = 7.91, 7.83 Hz, 1H), 7.47 (dd, J = 7.89, 1.55 Hz, 2H), 7.38−7.27 (m, 3H), 6.97 (d, J = 8.30 Hz, 1H), 6.69 (dd, J = 8.30, 1.83 Hz, 1H), 6.59 (d, J = 1.83 Hz, 1H), 4.07 (t, J = 6.81 Hz, 2H), 3.97 (s, 3H), 3.79 (s, 3H), 1.89 (dt, J = 7.02, 6.81 Hz, 2H), 1.54−1.44 (m, 2H), 1.40−1.23 (m, 24H), 0.88 (t, J = 6.40 Hz, 3H); ^{13}C NMR (75 MHz, $CDCl_3$) δ 165.43, 154.98, 150.25, 149.99, 139.14, 136.45, 134.07, 131.96, 131.30, 130.02, 129.28, 129.08, 128.22, 127.80, 122.48, 121.08, 113.03, 111.23, 69.11, 56.13, 52.63, 31.93, 29.70, 29.62, 29.59, 29.41, 29.36, 29.05, 25.98, 22.70, 14.13; MS (ESI) *m*/*z* 664 (M^+); Anal. ($C_{38}H_{52}N_2O_6S$) calcd, C, 68.64; H, 7.88; N, 4.21; found, C, 68.66; H, 7.93; N, 4.22. Compound **29Z**: mp 75−77 °C; ^{1}H NMR (300 MHz, $CDCl_3$) δ 8.66 (dd, J = 1.61, 1.54 Hz, 1H), 8.27 (ddd, J = 7.70, 2.94, 1.61 Hz, 1H), 8.16 (ddd, J = 7.90, 2.94, 1.54 Hz, 1H), 7.63 (dd, J = 7.90, 7.70 Hz, 1H), 7.54−7.49 (m, 3H), 7.47 (brs, 1H), 7.29 (d, J = 1.80 Hz, 1H), 7.13−7.10 (m,

2H), 6.68 (d, J = 8.39 Hz, 1H), 6.63 (dd, J = 8.39, 1.80 Hz, 1H), 3.97 (t, J = 6.99 Hz, 2H), 3.95 (s, 3H), 3.86 (s, 3H), 1.81 (dt, J = 7.70, 6.58 Hz, 2H), 1.46−1.44 (m, 2H), 1.40−1.21 (m, 24H), 0.88 (t, J = 6.37 Hz, 3H); ^{13}C NMR (75 MHz, $CDCl_3$) δ 165.38, 155.01, 150.65, 149.20, 146.37, 139.14, 134.07, 131.90, 131.29, 131.05, 130.16, 129.73, 129.23, 128.82, 128.27, 122.17, 111.30, 109.43, 68.94, 55.93, 52.61, 31.93, 29.69, 29.59, 29.54, 29.37, 28.99, 25.90, 22.70, 14.13; MS (ESI) m/z 664 (M^+); Anal. ($C_{38}H_{52}N_2O_6S$) calcd, C, 68.64; H, 7.88; N, 4.21; found, C, 68.73; H, 7.99; N, 4.05.

(*E*)-5-[1-(4-Cetyloxy-3-methoxyphenyl)-1-phenylmethylene]-sulfohydrazono isophthalic Acid (30E). To a solution of **25E** (108 mg, 0.15 mmol) in THF (3 mL) and methanol (1 mL) was added 1 N NaOH (1 mL). The mixture was stirred for 19 h, diluted with $CHCl_3$, washed with 1 N hydrochloric acid and brine, dried over Na_2SO_4, filtered, and concentrated. Recrystallization from isopropyl alcohol gave **30E** as a pale yellow powder (97 mg, 93%). mp 161−163 °C; ^{1}H NMR (300 MHz, DMSO-d_6) δ 13.82 (brs, 2H), 10.65 (brs, 1H), 8.65 (s, 3H), 7.43−7.30 (m, 5H), 7.06 (d, J = 8.80 Hz, 1H), 6.77−6.73 (m, 2H), 3.99 (t, J = 6.54 Hz, 2H), 3.69 (s, 3H), 1.73 (dt, J = 7.09, 6.54 Hz, 2H), 1.42−1.19 (m, 26H), 0.83 (t, J = 7.09 Hz, 3H); ^{13}C NMR (75 MHz, DMSO-d_6) δ 165.42, 155.66, 149.16, 148.72, 139.78, 137.29, 133.63, 132.28, 132.14, 129.91, 128.26, 127.70, 124.18, 121.98, 112.57, 112.43, 68.11, 55.62, 31.32, 29.07, 28.77, 28.74, 25.58, 22.12, 13.98; MS (ESI) m/z 693 (MH^-); Anal. ($C_{38}H_{50}N_2O_8S$) calcd, C, 65.68; H, 7.25; N, 4.03; found, C, 65.90; H, 7.36; N, 3.98.

(*Z*)-5-[1-(4-Cetyloxy-3-methoxyphenyl)-1-phenylmethylene]-sulfohydrazono isophthalic Acid (30Z). Compound **30Z** was prepared according to the procedure described for **30E** but with **25Z** instead of **25E**. Compound **30Z** was obtained as a colorless powder (53 mg, 85%). mp 179−181 °C; ^{1}H NMR (300 MHz, DMSO-d_6) δ 13.81 (brs, 2H), 10.44 (brs, 1H), 8.65 (s, 3H), 7.51−7.49 (m, 2H), 7.23−7.19 (m, 2H), 7.10 (d, J = 1.71 Hz, 1H), 6.82 (d, J = 8.32 Hz, 1H), 6.45 (dd, J = 8.32, 1.71 Hz, 2H), 3.90 (t, J = 6.51 Hz, 2H), 3.68 (s, 3H), 1.66 (dt, J = 6.59, 6.41 Hz, 2H), 1.38−1.16 (m, 26H), 0.83 (t, J = 7.09 Hz, 3H); ^{13}C NMR (75 MHz, DMSO-d_6) δ 165.43, 156.57, 150.05, 148.65, 139.74, 133.64, 132.53, 132.35, 132.23, 129.42, 129.14, 128.91, 128.56, 122.05, 111.65, 108.62, 68.07, 55.04, 31.29, 29.02, 28.95, 28.70, 28.57, 25.43, 22.09, 13.96; MS (ESI) m/z 693 (MH^-); Anal. ($C_{38}H_{50}N_2O_8S$) calcd, C, 65.68; H, 7.25; N, 4.03; found, C, 65.89; H, 7.32; N, 3.97.

(*E*)-5-[1-(4-Octyloxy-3-methoxyphenyl)-1-phenylmethylene]-sulfohydrazono isophthalic Acid (31E). Compound **31E** was prepared according to the procedure described for **30E**, but with **26E** instead of **25E**. Compound **31E** was obtained as a pale yellow powder (231 mg, 82%). mp 190−192 °C; ^{1}H NMR (300 MHz, DMSO-d_6) δ 10.65 (brs, 1H), 8.66 (s, 3H), 7.41−7.32 (m, 5H), 7.07 (d, J = 8.81 Hz, 1H), 6.77−6.75 (m, 2H), 4.01 (t, J = 6.42 Hz, 2H), 3.70 (s, 3H), 1.75 (dt, J = 6.42, 6.06 Hz, 2H), 1.44−1.42 (m, 2H), 1.40−1.24 (m, 8H), 0.87 (t, J = 6.97 Hz, 3H); ^{13}C NMR (75 MHz, DMSO-d_6) δ 165.47, 155.68, 149.17, 148.71, 139.77, 137.31, 133.69, 132.33,132.17,129.95, 128.30, 127.74, 124.19, 122.02, 112.55, 112.40, 68.12, 55.64, 31.32, 28.75, 25.62, 22.15, 14.04; MS (ESI) m/z 581 (MH^-); Anal. ($C_{30}H_{34}N_2O_8S$) calcd, C, 61.84; H, 5.88; N, 4.81; found, C, 62.00; H, 5.88; N, 4.68.

(*Z*)-5-[1-(4-Octyloxy-3-methoxyphenyl)-1-phenylmethylene]-sulfohydrazono isophthalic Acid (31Z). Compound **31Z** was prepared according to the procedure described for **30E** but with **26Z** instead of **25E**. Compound **31Z** was obtained as a colorless powder (421 mg, 91%). mp 209−210 °C; ^{1}H NMR (300 MHz, DMSO-d_6) δ 10.44 (brs, 1H), 8.66 (s, 3H), 7.52−7.50 (m, 3H), 7.24−7.21 (m, 2H), 7.11 (d, J = 2.02 Hz, 1H), 6.84 (d, J = 8.44 Hz, 1H), 6.47 (dd, J = 8.44, 2.02 Hz, 1H), 3.92 (t, J = 6.61 Hz, 2H), 3.69 (s, 3H), 1.68 (dt, J = 7.34, 6.61 Hz, 2H), 1.40−1.22 (m, 10H), 0.85 (m, 3H); ^{13}C NMR (75 MHz, DMSO-d_6) δ 165.46, 156.61, 150.06, 148.67, 139.74, 133.68, 132.55, 132.37, 132.25, 129.44, 129.14, 128.94, 128.58, 122.08, 111.66, 108.61, 68.09, 55.05, 31.25, 28.71, 28.65, 28.59, 25.48, 22.09, 13.99; MS (ESI) m/z 581 (MH^-); Anal. ($C_{30}H_{34}N_2O_8S$) calcd, C, 61.84; H, 5.88; N, 4.81; found, C, 61.65; H, 5.82; N, 4.71.

(*E*)-5-[1-(4-Butyloxy-3-methoxyphenyl)-1-phenylmethylene]-sulfohydrazono isophthalic Acid (32E). Compound **32E** was prepared according to the procedure described for **30E** but with **27E** instead of **25E**. Compound **32E** was obtained as a colorless powder (632 mg, 92%). mp 196−199 °C; ^{1}H NMR (300 MHz, DMSO-d_6) δ 10.65 (brs, 1H), 8.66 (s, 3H), 7.39−7.32 (m, 5H), 7.08 (d, J = 8.81 Hz, 1H), 6.77−6.74 (m, 2H), 4.02 (t, J = 6.42 Hz, 2H), 3.71 (s, 3H), 1.73 (dt, J = 6.79, 6.42 Hz, 2H), 1.49−1.42 (m, 2H), 0.95 (t, J = 7.34 Hz, 3H); ^{13}C NMR (75 MHz, DMSO-d_6) δ 165.41, 155.68, 149.16, 148.71, 139.77, 137.28, 133.62, 132.26, 132.14, 129.92, 128.27, 127.70, 124.17, 121.98, 112.55, 112.41, 67.77, 55.62, 30.76, 18.79, 13.69; MS (ESI) m/z 525 (MH^-); Anal. ($C_{26}H_{26}N_2O_8S$) calcd, C, 59.31; H, 4.98; N, 5.32; found, C, 58.99; H, 4.93; N, 5.16.

(*E*)-5-[1-(4-Cetyloxyphenyl)-1-phenylmethylene]sulfohydrazono isophthalic Acid (33E). Compound **33E** was prepared according to the procedure described for **30E** but with **28E** instead of **25E**. Compound **33E** was obtained as a pale yellow powder (13 mg, 26%). mp 175−176 °C; ^{1}H NMR (300 MHz, DMSO-d_6) δ 13.82 (brs, 2H), 10.64 (brs, 1H), 8.66 (brs, 3H), 7.42−7.26 (m, 5H), 7.17 (d, J = 7.71 Hz, 2H), 7.03 (d, J = 7.71 Hz, 2H), 4.01 (t, J = 6.40 Hz, 2H), 1.73−1.69 (m, 2H), 1.46−1.14 (m, 26H), 0.84 (t, J = 6.71 Hz, 3H); ^{13}C NMR (75 MHz, DMSO-d_6) δ 165.38, 159.52, 155.92, 139.62, 137.45, 132.20, 130.65, 128.23, 127.72, 124.16, 114.46, 67.56, 31.26, 29.01, 28.98, 28.71, 28.67, 28.58, 25.48, 22.06, 13.93; MS (ESI) m/z 663 (MH^-); Anal. ($C_{37}H_{48}N_2O_7S$) calcd, C, 66.84; H, 7.28; N, 4.21; found, C, 66.73; H, 7.50; N, 4.29.

(*E*)-3-[1-(4-Cetyloxy-3-methoxyphenyl)-1-phenylmethylene]-sulfohydrazono benzoic Acid (34E). Compound **34E** was prepared according to the procedure described for **30E**, but with **29E** instead of **25E**. Compound **34E** was obtained as a colorless powder (54 mg, 83%). mp 134−135 °C; ^{1}H NMR (300 MHz, DMSO-d_6) δ 13.50 (brs, 1H), 10.56 (brs, 1H), 8.50 (s, 1H), 8.20 (d, J = 7.83 Hz, 1H), 8.13 (d, J = 7.72 Hz, 1H), 7.77 (dd, J = 7.83, 7.72 Hz, 1H), 7.39−7.28 (m, 5H), 7.06 (d, J = 7.94 Hz, 1H), 6.74−6.72 (m, 2H), 4.00 (t, J = 6.30 Hz, 2H), 3.70 (s, 3H), 1.72 (dt, J = 6.80, 6.32 Hz, 2H), 1.45−1.19 (m, 26H), 0.84 (t, J = 6.80 Hz, 3H); ^{13}C NMR (75 MHz, DMSO-d_6) δ 166.11, 154.98, 149.06, 148.76, 139.35, 137.32, 133.45, 131.64, 131.53, 129.75, 129.66, 128.64, 128.26, 127.55, 124.28, 121.85, 112.63, 112.37, 68.09, 55.60, 31.30, 29.06, 28.71, 25.57, 22.10, 13.97; MS (ESI) m/z 649 (MH^-); Anal. ($C_{37}H_{50}N_2O_6S$) calcd, C, 68.28; H, 7.74; N, 4.30; found, C, 68.23; H, 7.80; N, 4.25.

(*Z*)-3-[1-(4-Cetyloxy-3-methoxyphenyl)-1-phenylmethylene]-sulfohydrazono benzoic Acid (34Z). Compound **34Z** was prepared according to the procedure described for **30E**, but with **29Z** instead of **25E**. Compound **34Z** was obtained as a colorless powder (45 mg, 69%). mp 72−74 °C; ^{1}H NMR (300 MHz, DMSO-d_6) δ 13.49 (brs, 1H), 10.37 (brs, 1H), 8.49 (s, 1H), 8.20 (d, J = 7.80 Hz, 1H), 8.14 (d, J = 7.69 Hz, 1H), 7.76 (dd, J = 7.80, 7.69 Hz, 1H), 7.51−7.49 (m, 3H), 7.22−7.19 (m, 2H), 7.04 (d, J = 1.78 Hz, 1H), 6.82 (d, J = 8.37 Hz, 1H), 6.47 (dd, J = 8.37, 1.78 Hz, 1H), 3.90 (t, J = 6.42 Hz, 2H), 3.67 (s, 3H), 1.67 (dt, J = 6.57, 6.42 Hz, 2H), 1.38−1.17 (m, 26H), 0.84 (t, J = 6.82 Hz, 3H); ^{13}C NMR (75 MHz, DMSO-d_6) δ 166.14, 149.93, 148.59, 139.20, 137.09, 133.48, 132.61, 131.98, 131.48, 129.52, 129.37, 128.95, 128.81, 128.57, 122.31, 121.79, 111.71, 108.99, 68.08, 55.13, 31.29, 29.02, 28.96, 28.70, 28.57, 25.44, 22.10, 13.97; MS (ESI) m/z 649 (MH^-); Anal. ($C_{37}H_{50}N_2O_6S$) calcd, C, 68.28; H, 7.74; N, 4.30; found, C, 68.30; H, 7.80; N, 4.28.

Acknowledgment. We thank Ms. Y. Kato, Ms. A. Furukawa, and Ms. Y. Hironaka at TOA EIYO Ltd. for their dedicated technical assistance and Accelrys K.K., Japan, for providing excellent technical support. This study was supported by a research grant for 'Research on Health Sciences Focusing on Drug Innovation' (KH21004) from the Japan Health Sciences Foundation and by a Grant-in-Aid for Scientific Research on Priority Areas (A) "Exploitation of Multi-Element Cyclic

Molecules" from the Ministry of Education, Culture, Sports, Science and Technology, Japan.

Supporting Information Available: One hundred seven structures in the database for assessing the GH score and the structures of 36 assayed compounds. All elemental analyses (C, H, N) for synthesized compounds. This material is available free of charge via the Internet at http://pubs.acs.org.

References

(1) Saba, J. D.; Hla, T. Point-counterpoint of sphingosine 1-phosphate metabolism. *Circ. Res.* **2004**, *94* (6), 724−34.

(2) Spiegel, S.; Milstien, S. Sphingosine-1-phosphate: an enigmatic signalling lipid. *Nat. Rev. Mol. Cell Biol.* **2003**, *4* (5), 397−407.

(3) Hla, T.; Maciag, T. An abundant transcript induced in differentiating human endothelial cells encodes a polypeptide with structural similarities to G-protein-coupled receptors. *J. Biol. Chem.* **1990**, *265* (16), 9308−13.

(4) Chun, J.; Goetzl, E. J.; Hla, T.; Igarashi, Y.; Lynch, K. R.; Moolenaar, W.; Pyne, S.; Tigyi, G. International Union of Pharmacology. XXXIV. Lysophospholipid receptor nomenclature. *Pharmacol. Rev.* **2002**, *54* (2), 265−9.

(5) Lee, O. H.; Kim, Y. M.; Lee, Y. M.; Moon, E. J.; Lee, D. J.; Kim, J. H.; Kim, K. W.; Kwon, Y. G. Sphingosine 1-phosphate induces angiogenesis: its angiogenic action and signaling mechanism in human umbilical vein endothelial cells. *Biochem. Biophys. Res. Commun.* **1999**, *264* (3), 743−50.

(6) Wang, F.; Van Brocklyn, J. R.; Hobson, J. P.; Movafagh, S.; Zukowska-Grojec, Z.; Milstien, S.; Spiegel, S. Sphingosine 1-phosphate stimulates cell migration through a G (i)-coupled cell surface receptor. Potential involvement in angiogenesis. *J. Biol. Chem.* **1999**, *274* (50), 35343−50.

(7) Paik, J. H.; Chae, S.; Lee, M. J.; Thangada, S.; Hla, T. Sphingosine 1-phosphate-induced endothelial cell migration requires the expression of EDG-1 and EDG-3 receptors and Rho-dependent activation of alpha vbeta3- and beta1-containing integrins. *J. Biol. Chem.* **2001**, *276* (15), 11830−7.

(8) Kwon, Y. G.; Min, J. K.; Kim, K. M.; Lee, D. J.; Billiar, T. R.; Kim, Y. M. Sphingosine 1-phosphate protects human umbilical vein endothelial cells from serum-deprived apoptosis by nitric oxide production. *J. Biol. Chem.* **2001**, *276* (14), 10627−33.

(9) Waeber, C.; Blondeau, N.; Salomone, S. Vascular sphingosine-1-phosphate S1P1 and S1P3 receptors. *Drug News Perspect.* **2004**, *17* (6), 365−82.

(10) Alewijnse, A. E.; Peters, S. L.; Michel, M. C. Cardiovascular effects of sphingosine-1-phosphate and other sphingomyelin metabolites. *Br. J. Pharmacol.* **2004**, *143* (6), 666−84.

(11) Watterson, K. R.; Ratz, P. H.; Spiegel, S. The role of sphingosine-1-phosphate in smooth muscle contraction. *Cell. Signal.* **2005**, *17* (3), 289−98.

(12) McVerry, B. J.; Garcia, J. G. In vitro and in vivo modulation of vascular barrier integrity by sphingosine 1-phosphate: mechanistic insights. *Cell. Signal.* **2005**, *17* (2), 131−9.

(13) Aki, F. T.; Kahan, B. D. FTY720: A new kid on the block for transplant immunosuppression. *Expert Opin. Biol. Ther.* **2003**, *3* (4), 665−81.

(14) Mandala, S.; Hajdu, R.; Bergstrom, J.; Quackenbush, E.; Xie, J.; Milligan, J.; Thornton, R.; Shei, G. J.; Card, D.; Keohane, C.; Rosenbach, M.; Hale, J.; Lynch, C. L.; Rupprecht, K.; Parsons, W.; Rosen, H. Alteration of lymphocyte trafficking by sphingosine-1-phosphate receptor agonists. *Science* **2002**, *296* (5566), 346−9.

(15) Brinkmann, V.; Davis, M. D.; Heise, C. E.; Albert, R.; Cottens, S.; Hof, R.; Bruns, C.; Prieschl, E.; Baumruker, T.; Hiestand, P.; Foster, C. A.; Zollinger, M.; Lynch, K. R. The immune modulator FTY720 targets sphingosine 1-phosphate receptors. *J. Biol. Chem.* **2002**, *277* (24), 21453−7.

(16) Matloubian, M.; Lo, C. G.; Cinamon, G.; Lesneski, M. J.; Xu, Y.; Brinkmann, V.; Allende, M. L.; Proia, R. L.; Cyster, J. G. Lymphocyte egress from thymus and peripheral lymphoid organs is dependent on S1P receptor 1. *Nature* **2004**, *427* (6972), 355−60.

(17) Budde, K.; Schmouder, R. L.; Brunkhorst, R.; Nashan, B.; Lucker, P. W.; Mayer, T.; Choudhury, S.; Skerjanec, A.; Kraus, G.; Neumayer, H. H. First human trial of FTY720, a novel immunomodulator, in stable renal transplant patients. *J. Am. Soc. Nephrol.* **2002**, *13* (4), 1073−83.

(18) Bunemann, M.; Brandts, B.; zu Heringdorf, D. M.; van Koppen, C. J.; Jakobs, K. H.; Pott, L. Activation of muscarinic K+ current in guinea-pig atrial myocytes by sphingosine-1-phosphate. *J. Physiol. (London)* **1995**, *489* (Pt 3), 701−7.

(19) Guo, J.; MacDonell, K. L.; Giles, W. R. Effects of sphingosine 1-phosphate on pacemaker activity in rabbit sino-atrial node cells. *Pflugers Arch.* **1999**, *438* (5), 642−8.

(20) Himmel, H. M.; Meyer Zu Heringdorf, D.; Graf, E.; Dobrev, D.; Kortner, A.; Schuler, S.; Jakobs, K. H.; Ravens, U. Evidence for Edg-3 receptor-mediated activation of I(K.ACh) by sphingosine-1-phosphate in human atrial cardiomyocytes. *Mol. Pharmacol.* **2000**, *58* (2), 449−54.

(21) Forrest, M.; Sun, S. Y.; Hajdu, R.; Bergstrom, J.; Card, D.; Doherty, G.; Hale, J.; Keohane, C.; Meyers, C.; Milligan, J.; Mills, S.; Nomura, N.; Rosen, H.; Rosenbach, M.; Shei, G. J.; Singer, II; Tian, M.; West, S.; White, V.; Xie, J.; Proia, R. L.; Mandala, S. Immune cell regulation and cardiovascular effects of sphingosine 1-phosphate receptor agonists in rodents are mediated via distinct receptor subtypes. *J. Pharmacol. Exp. Ther.* **2004**, *309* (2), 758−68.

(22) Sanna, M. G.; Liao, J.; Jo, E.; Alfonso, C.; Ahn, M. Y.; Peterson, M. S.; Webb, B.; Lefebvre, S.; Chun, J.; Gray, N.; Rosen, H. Sphingosine 1-phosphate (S1P) receptor subtypes S1P1 and S1P3, respectively, regulate lymphocyte recirculation and heart rate. *J. Biol. Chem.* **2004**, *279* (14), 13839−48.

(23) Jolly, P.; Rosenfeldt, H.; Milstien, S.; Spiegel, S. The roles of sphingosine-1-phosphate in asthma. *Mol. Immunol.* **2002**, *38* (16−18), 1239.

(24) Hale, J. J.; Doherty, G.; Toth, L.; Mills, S. G.; Hajdu, R.; Keohane, C. A.; Rosenbach, M.; Milligan, J.; Shei, G. J.; Chrebet, G.; Bergstrom, J.; Card, D.; Forrest, M.; Sun, S. Y.; West, S.; Xie, H.; Nomura, N.; Rosen, H.; Mandala, S. Selecting against S1P3 enhances the acute cardiovascular tolerability of 3-(N-benzyl)aminopropylphosphonic acid S1P receptor agonists. *Bioorg. Med. Chem. Lett.* **2004**, *14* (13), 3501−5.

(25) Li, Z.; Chen, W.; Hale, J. J.; Lynch, C. L.; Mills, S. G.; Hajdu, R.; Keohane, C. A.; Rosenbach, M. J.; Milligan, J. A.; Shei, G. J.; Chrebet, G.; Parent, S. A.; Bergstrom, J.; Card, D.; Forrest, M.; Quackenbush, E. J.; Wickham, L. A.; Vargas, H.; Evans, R. M.; Rosen, H.; Mandala, S. Discovery of Potent 3,5-Diphenyl-1,2,4-oxadiazole Sphingosine-1-phosphate-1 (S1P(1)) Receptor Agonists with Exceptional Selectivity against S1P(2) and S1P(3). *J. Med. Chem.* **2005**, *48* (20), 6169−73.

(26) Parrill, A. L.; Sardar, V. M.; Yuan, H. Sphingosine 1-phosphate and lysophosphatidic acid receptors: agonist and antagonist binding and progress toward development of receptor-specific ligands. *Semin. Cell Dev. Biol.* **2004**, *15* (5), 467−76.

(27) Dunn, P. M.; Blakeley, A. G. Suramin: a reversible P2-purinoceptor antagonist in the mouse vas deferens. *Br. J. Pharmacol.* **1988**, *93* (2), 243−5.

(28) Ullmann, H.; Meis, S.; Hongwiset, D.; Marzian, C.; Wiese, M.; Nickel, P.; Communi, D.; Boeynaems, J. M.; Wolf, C.; Hausmann, R.; Schmalzing, G.; Kassack, M. U. Synthesis and Structure-Activity Relationships of Suramin-Derived P2Y(11) Receptor Antagonists with Nanomolar Potency. *J. Med. Chem.* **2005**, *48* (22), 7040−7048.

(29) Bojanowski, K.; Lelievre, S.; Markovits, J.; Couprie, J.; Jacquemin-Sablon, A.; Larsen, A. K. Suramin is an inhibitor of DNA topoisomerase II in vitro and in Chinese hamster fibrosarcoma cells. *Proc. Natl. Acad. Sci. U.S.A.* **1992**, *89* (7), 3025−9.

(30) De Clercq, E. Suramin: a potent inhibitor of the reverse transcriptase of RNA tumor viruses. *Cancer Lett.* **1979**, *8* (1), 9−22.

(31) Beindl, W.; Mitterauer, T.; Hohenegger, M.; Ijzerman, A. P.; Nanoff, C.; Freissmuth, M. Inhibition of receptor/G protein coupling by suramin analogues. *Mol. Pharmacol.* **1996**, *50* (2), 415−23.

(32) Davis, M. D.; Clemens, J. J.; Macdonald, T. L.; Lynch, K. R. Sphingosine 1-phosphate analogs as receptor antagonists. *J. Biol. Chem.* **2005**, *280* (11), 9833−41.

(33) Lynch, K.; Macdonald, T. L. Orally available sphingosine 1-phosphate receptor agonists and antagonists. WO2005041899, 2005.

(34) Böhm, H.-J.; Alexander Flohr, A.; Stahl, M. Scaffold hopping *Drug Discovery Today: Technol.* **2004**, *1* (3), 217−224.

(35) Bleicher, K. H.; Green, L. G.; Martin, R. E.; Rogers-Evans, M. Ligand identification for G-protein-coupled receptors: a lead generation perspective. *Curr. Opin. Chem. Biol.* **2004**, *8* (3), 287−96.

(36) Koide, Y.; Hasegawa, T.; Takahashi, A.; Endo, A.; Mochizuki, N.; Nakagawa, M.; Nishida, A. Development of novel EDG3 antagonists using a 3D database search and their structure-activity relationships. *J. Med. Chem.* **2002**, *45* (21), 4629−38.

(37) Jongsma, M.; Hendriks-Balk, M. C.; Michel, M. C.; Peters, S. L.; Alewijnse, A. E. BML-241 fails to display selective antagonism at the sphingosine-1-phosphate receptor, S1P(3). *Br. J. Pharmacol.* **2006**, *149* (3), 277−82.

(38) Clement, O. O.; Mehl, A. T. HipHop: Pharmacophores Based on Multiple Common-Feature Alignments. In *Pharmacophore Perception, Development, and Use in Drug Design*, 1st ed.; Güner, O. F., Ed.; IUL Biotechnology Series: La Jolla, CA, 2000; pp 69−84.

(39) Güner, O. F.; Henry, D. R. Metric for Analyzing Hit Lists and Pharmacophores. In *Pharmacophore Perception, Development, and Use in Drug Design*, 1st ed.; Güner, O. F., Ed.; IUL Biotechnology Series: La Jolla, CA, 2000; pp 191−212.

(40) Güner, O. F.; Waldman, M.; Hoffmann, D.; Kim, J. H. Strategies for Database Mining and Pharmacophore Development. In *Pharmacophore Perception, Development, and Use in Drug Design*, 1st ed.; Güner, O. F., Ed.; IUL Biotechnology Series: La Jolla, CA, 2000; pp 213−236.
(41) Clement, O. O.; Freeman, C. M.; Hartmann, R. W.; Handratta, V. D.; Vasaitis, T. S.; Brodie, A. M.; Njar, V. C. Three dimensional pharmacophore modeling of human CYP17 inhibitors. Potential agents for prostate cancer therapy. *J. Med. Chem.* **2003**, *46* (12), 2345−51.
(42) Gillner, M.; Greenidge, P. The Use of Multiple Excluded Volumes Derived from X-Ray Crystallographic Structures in 3D Database Searching and 3D QSAR. In *Pharmacophore Perception, Development, and Use in Drug Design*, 1st ed.; Güner, O. F., Ed.; IUL Biotechnology Series: La Jolla, CA, 2000; pp 371−384.
(43) Burk, M. J.; Martinez, J. P.; Feaster, J. E.; Cosford, N. Catalytic, asymmetric reductive amination of ketones via highly enantioselective hydrogenation of the C=N double bond. *Tetrahedron* **1994**, *50*, 4399−4428.
(44) Györgydeák, Z.; Holzer, W. Acylation, of Guanylhydrazones Derived from Cyclic Ketones: Synthesis of 3-Acylamino-1-cycloalkenyl-5-methyl-1H-1,2,4-triazoles. *Heterocycles* **1998**, *48*, 1395−1406.
(45) Hawkes, G. E.; Herwig, K.; Roberts, J. D. Nuclear, magnetic resonance spectroscopy. Use of carbon-13 spectra to establish configurations of oximes. *J. Org. Chem.* **1974**, *39*, 1017−1028.
(46) Levy, G. C.; Gordon, L. Nelson, G. L. Carbon-13 NMR study of aliphatic amides and oximes. Spin-lattice relaxation times and fast internal motions. *J. Am. Chem. Soc.* **1972**, *94*, 4897−4901.
(47) Qin, J.; Friestad, G. K. Stereocontrol, in hydride addition to ketone-derived chiral N-acylhydrazones. *Tetrahedron* **2003**, *59*, 6393−6402.
(48) Roberts, J. D.; Grutzner, J. B.; Jautelat, M.; Dence, J. B.; Smith, R. A. Nuclear magnetic resonance spectroscopy. Carbon-13 chemical shifts in norbornyl derivatives. *J. Am. Chem. Soc.* **1970**, *92*, 7107−7120.
(49) Dalling, D. K.; Grant, D. M. Carbon-13 magnetic resonance. IX. Methylcyclohexanes. *J. Am. Chem. Soc.* **1967**, *89*, 6612−6622.
(50) Grant, D. M.; Cheney, B. V. Carbon-13 magnetic resonance. VII. Steric perturbation of the carbon-13 chemical shift. *J. Am. Chem. Soc.* **1967**, *89*, 5315−5318.
(51) Clemens, J. J.; Davis, M. D.; Lynch, K. R.; Macdonald, T. L. Synthesis of 4(5)-phenylimidazole-based analogues of sphingosine-1-phosphate and FTY720: discovery of potent S1P1 receptor agonists. *Bioorg. Med. Chem. Lett.* **2005**, *15* (15), 3568−72.
(52) Clemens, J. J.; Davis, M. D.; Lynch, K. R.; Macdonald, T. L. Synthesis of para-alkyl aryl amide analogues of sphingosine-1-phosphate: discovery of potent S1P receptor agonists. *Bioorg. Med. Chem. Lett.* **2003**, *13* (20), 3401−4.
(53) Catalyst, 4.9; Accelrys: CA. (Web Site: http://www.accelrys.com/products/catalyst/).
(54) MDL Assay Explorer, Elsevier MDL: CA. (Web Site: http://www.mdl.com/products/experiment/assay_explorer/index.jsp).
(55) Criodain, T. O.; OSullivan, M.; Meegan, M. J.; Donnelly, D. M. X. Latinone, A Phenanthrene-1,4-Quinone From *Dalbergia latifolia*. *Phytochemistry* **1981**, *20*, 1089−1092.

JM060834D